Nonlinear Dynamics (2005) 41: 69–110

Advanced Proper Orthogonal Decomposition Tools: Using Reduced Order Models to Identify Normal Modes of Vibration and Slow Invariant Manifolds in the Dynamics of Planar Nonlinear Rods

IOANNIS GEORGIOU

National Technical University of Athens, P.O. Box 640-33 Zografos 157 10, Athens, Greece; Present address: SAIC, McLean, VA 22102, U.S.A.; (e-mail: georgiou@central.ntua.gr; ioannis.t.georgiou@saic.com; fax: +11-30-210-7721117)

(Received: 14 May 2004; accepted: 29 September 2004)

Abstract. Reduced order models for the dynamics of geometrically exact planar rods are derived by projecting the nonlinear equations of motion onto a subspace spanned by a set of proper orthogonal modes. These optimal modes are identified by a proper orthogonal decomposition processing of high-resolution finite element dynamics. A three-degree-of-freedom reduced system is derived to study distinct categories of motions dominated by a single POD mode. The modal analysis of the reduced system characterizes in a unique fashion for these motions, since its linear natural frequencies are near to the natural frequencies of the full-order system. For free motions characterized by a single POD mode, the eigen-vector matrix of the derived reduced system coincides with the principal POD-directions. This property reflects the existence of a normal mode of vibration, which appears to be close to a slow invariant manifold. Its shape is captured by that of the dominant POD mode. The modal analysis of the POD-based reduced order system provides a potentially valuable tool to characterize the spatio-temporal complexity of the dynamics in order to elucidate connections between proper orthogonal modes and nonlinear normal modes of vibration.

Key words: coupled vibrations, geometric singular perturbations, normal modes of vibration, proper orthogonal decomposition, reduced order system, slow invariant manifolds

1. Introduction

This paper deals with the derivation of reduced order models of highly nonlinear coupled systems in structural mechanics. The prototypical system we consider is a geometrically exact elastic rod. Reduced order modes are based on the knowledge of POD modes computed by POD of the finite element approximation considered to be a database of information on the dynamics of the trajectory of a motion. The reduced order models are used to pave the way towards a normal mode characterization of coupled vibrations. The basic issue that will be addressed is when POD modes represent normal modes of vibration. Such a connection is necessary to develop POD-based techniques to characterize vibrations of coupled systems with complicated domains.

It is well-known that the concept of normal mode of vibration [1–5] plays a fundamental role in analyzing (dimension reduction and decoupling) the dynamics of vibratory systems in mechanics. A basic result is the fact that a local normal mode of vibration manifests itself as a local two-dimensional invariant manifold in phase space of the dynamics [6, 7]. The invariance of the manifold leads naturally to the lowest possible reduction (a modal oscillator) of the system dimension. Another basic result is the fact that the linearization of a multi-degree-of-freedom nonlinear vibratory system is decomposed into a complete set of orthogonal normal modes (linear invariant manifolds). Still another basic result is the significant role the linear normal modes play in reducing the dimension of a system to capture its dominant degrees-of-freedom: projection of the original nonlinear system onto subspaces spanned

by the linearized normal modes, the classical Galerkin method, reduces the dimension of a system. But this reduction is not optimal since the projection is not onto the invariant subspaces representing the normal modes of vibration. Clearly projection of the system onto its normal modes should yield an optimal reduced model. This is not an easy task since the normal modes of a nonlinear system, and in particular a distributed one composed of coupled multi-fields, cannot be computed analytically given the present state-of-art of analytical methods (usually perturbation techniques of linear theory) of nonlinear systems.

It is not an accident that most of the work, reported in the literature, on normal modes and model reduction of continuous systems concerns classical nonlinear models of structural elements (beams, plates and shells). These models possess low-order complexity in regards to the mathematical structure of coupling among various fields since they are derived from continuum mechanics models (three-dimensional elasticity), which are exact, by reducing the dimension of the physical domain and simplifying the nonlinearities. These assumptions result in a considerable loss of information for motions away from equilibrium. If the exact nature of coupling among the various fields and nonlinearities must be kept intact, a finite element representation of the system should be used to compute accurately the normal modes of vibration. In a recent work, Mazzilli [8] presents an interesting approach to compute the normal modes and derive reduced models for a finite element model of a planar frame.

Given the tremendous impact of information technology (rapid computation, data processing and visualization) on computational mechanics, the issue of computing the normal modes of vibration of a coupled structural system should be addressed at the level of a finite element model of the system. For vibratory systems with arbitrary three-dimensional physical domains, the most accurate model that describes as precisely as desired the dynamics is a finite element model based on modern theory of rational continuum mechanics [9, 10]. The current state-of-art of computational mechanics algorithms and computer technology furnish effective tools for obtaining high-resolution information (numerical solutions) to the dynamics. This information should be processed properly to extract important underlining characteristics such as the shapes of the normal modes of vibration. The finite element dynamics can be characterized in an unparalleled way by means of proper orthogonal decompositions (POD). This technique decomposes optimally a specified segment of the trajectory of a motion into a set of proper orthogonal modes and it determines their auto-correlation energy content [11]. Recently, in the area of solid mechanics, Georgiou and Sansour [12] demonstrated how POD can be applied to analyze the finite element dynamics of geometrically exact elastic rods-coupled systems involving multi-field coupled dynamics. In view of the recent advances on POD processing of multi-field vibration data, the issue of normal modes of vibration for a nonlinear structural system involving coupled multi-fields can be addressed at the level of a finite element model for the system.

Characterization of the spatio-temporal complexity of the dynamics of multi-field structural systems can be addressed by determining normal modes of vibration and deriving reduced order models. The issue of normal modes of vibration and reduced models in coupled structural systems can be addressed by considering prototypical systems that model exactly the dominant nonlinearities. For rod and shell like structural systems, the most accurate models that capture exactly the dominant geometric nonlinearity and shearing effects are those describing exactly the displacement of the middle curve (surface) and the independent rotation of the cross-section. Relatively thick rod and shell-like structural systems can be modeled exactly as one and two-dimensional continua by means of the director-theory (Cosserat model) of continuum mechanics [13]. It is shown in Sansour and Bednarczyk [14] that the dynamics of these models can be computed accurately by means of finite element algorithms that preserve the total mechanical energy and momentum. Given the fact that the dynamics of these prototypical multi-field dynamical systems can be computed as accurately as desired and consequently characterized by POD, it

is not necessary to simplify the nonlinearities to address the issue of normal modes. On the contrary, this issue should be addressed at the level of the finite element representation of the system. A methodology is needed to tackle this issue.

Towards the development of a methodology to characterize systematically the spatio-temporal complexity of the dynamics of structural systems composed of coupled multi-fields, we derive reduced order models for the coupled equations of motion of geometrically exact rods by direct projection onto its proper orthogonal modes. The novel feature of this approach is the fact that the POD modes of a motion are extracted by POD processing of the dynamics of a finite element model [15]. It is known that, under certain conditions, POD modes of structural systems involving one-field dynamics represent normal modes of vibration [16]. For coupled structural systems composed of subsystems involving one-field dynamics, the underlining slow normal mode of vibration is realized as a pair of POD modes [17].

In this work, we apply POD to characterize aspects of the complexity of the dynamics of structural systems involving coupled multi-fields. In particular, we derive and analyze reduced order models based on POD analysis of the dynamics of finite element models of geometrically exact rods. In fluid mechanics, the POD method has been used to derive reduced models for the Navier–Stokes equations [18]. In solid mechanics, POD has been used to derive reduced models of a pipe carrying a fluid and is compared to other projection–reduction methods [19]. Moreover, POD has been used to explore the spatio-temporal dimensionality of the dynamics of a cable/mass system [20].

The paper is organized as follows. In Section 2, we present the equations of motion of a geometrically exact rod restricted to move in the plane. We consider this system to be a prototype for one-dimensional coupled structural systems to attempt to related proper orthogonal modes to nonlinear normal modes of vibration. In Section 3, we outline the method of proper orthogonal decompositions for coupled multi-field systems and point out the existence of motions of the rod dominated by a single POD mode. In Section 4, we derive reduced order models by direct projection of the coupled equations of motion of the rod onto a set of POD modes. In Section 5, we derive three degrees-of-freedom reduced models for motions dominated by a single POD mode. In Section 6, we outline the proper orthogonal decomposition-reduced model (POD-RM) method that we apply to extract the shape of a normal mode of vibration by analyzing a family of harmonically excited motions. In Section 7, we explore the properties of the mass, dissipation, and stiffness matrices of the reduced system by analyzing the free dynamics induced by a spatially uniform impulsive load. In Sections 8 and 9, we characterize systematically by means of the POD-RM tool a large number of harmonically forced motions to identify the shapes of some normal modes of the rod. In Section 10, we compare the reduced order system that generates the dynamics of the fundamental (first) normal mode of vibration to the full order system. In Section 11, we present evidence that the reduced order system derived from the POD structure of near resonant forced motions possesses a slow invariant manifold. Finally, in Section 12, we conclude and discuss the results concerning the relations between proper orthogonal modes and nonlinear normal modes of vibration.

2. Geometrically Exact Models in Structural Dynamics

We are going to derive reduced order models for geometrically exact dynamical systems in structural mechanics. The reduced models will provide us with advanced computational tools to determine relations between POD modes and normal modes of vibration in multi-field structural dynamical systems. In particular, we consider a geometrically exact model of an elastic rod. This model describes the dominant geometric nonlinearity exactly and thus accommodates coupling of the shearing of the cross-section to the displacement of the middle curve. Thus, this model possesses sufficient complexity in regards

to nonlinearity and number of coupled fields. In passing, it is worth mentioning that the geometrically exact model of a rod can be reduced to obtain the entire class of well-known linear models for beams, rings, and arches [21]. This is another reason justifying why this model is considered to be a prototypical dynamical system for our purpose.

The motion of the rod, modeled as one-dimensional Cosserat continuum, is described by the following set of coupled partial differential equations [22]:

$$\left.\begin{aligned}
&\rho A\frac{\partial^2 u_1(s,t)}{\partial t^2}+D\frac{\partial u_1(s,t)}{\partial t}\\
&\quad-\frac{A}{2}[E+G+(E-G)\cos(2\,\theta_3(s,t))]\frac{\partial^2 u_1(s,t)}{\partial s^2}\\
&\quad-\frac{A}{2}(E-G)\sin(2\,\theta_3(s,t))\frac{\partial^2 u_2(s,t)}{\partial s^2}-EA\sin(\theta_3(s,t))\frac{\partial\theta_3(s,t)}{\partial s}\\
&\quad-A(E-G)\left[-\sin(2\,\theta_3(s,t))\left(1+\frac{\partial u_1(s,t)}{\partial s}\right)+\cos(2\,\theta_3(s,t))\frac{\partial u_2(s,t)}{\partial s}\right]\frac{\partial\theta_3(s,t)}{\partial s}\\
&=F_1(s,t),
\end{aligned}\right\}\tag{1}$$

$$\left.\begin{aligned}
&\rho A\frac{\partial^2 u_2(s,t)}{\partial t^2}+D\frac{\partial u_2(s,t)}{\partial t}\\
&\quad-\frac{A}{2}(E-G)\sin(2\,\theta_3(s,t))\frac{\partial^2 u_1(s,t)}{\partial s^2}\\
&\quad-\frac{A}{2}[E+G+(E-G)\cos(2\,\theta_3(s,t))]\frac{\partial^2 u_2(s,t)}{\partial s^2}+EA\cos(\theta_3(s,t))\frac{\partial\theta_3(s,t)}{\partial s}\\
&\quad-A(E-G)\left[\cos(2\,\theta_3(s,t))\left(1+\frac{\partial u_1(s,t)}{\partial s}\right)+\sin(2\theta_3(s,t))\frac{\partial u_2(s,t)}{\partial s}\right]\frac{\partial\theta_3(s,t)}{\partial s}\\
&=F_2(s,t),
\end{aligned}\right\}\tag{2}$$

$$\left.\begin{aligned}
&\rho I\frac{\partial^2\theta_3(s,t)}{\partial t^2}+D\frac{\partial\theta_3(s,t)}{\partial t}-EI\frac{\partial^2\theta_3(s,t)}{\partial s^2}\\
&\quad-A[-E+(E-G)\cos(\theta_3(s,t))]\\
&\quad\times\left[\sin(\theta_3(s,t))\left(1+\frac{\partial u_1(s,t)}{\partial s}\right)-\cos(\theta_3(s,t))\frac{\partial u_2(s,t)}{\partial s}\right]\\
&\quad-(E-G)A\left[\left(\cos(\theta_3(s,t))\frac{\partial u_1(s,t)}{\partial s}+\sin(\theta_3(s,t))\frac{\partial u_2(s,t)}{\partial s}\right)\right]\\
&\quad\times\left[\sin(\theta_3(s,t))\left(1+\frac{\partial u_1(s,t)}{\partial s}\right)-\cos(\theta_3(s,t))\frac{\partial u_2(s,t)}{\partial s}\right]\\
&=M_1(s,t).
\end{aligned}\right\}\tag{3}$$

The independent variables s, t denote space and time, respectively. The dependent variables $u_1(s,t)$ and $u_2(s,t)$ denote respectively the longitudinal and transverse displacements of the neutral axis (middle curve); whereas the variable $\theta_3(s,t)$ denotes the in-plane rotational displacement of the cross-section. The constants L, A denote respectively the length of the rod and the area of its uniform rectangular cross-section. The constant I denotes the second moment of inertia of the cross-section. The material composing the rod is assumed to be linear elastic. The constants ρ, E, G, D denote respectively mass density, modulus of elasticity in extension and shearing, and coefficient of linear viscous damping. The

terms $F_1(s,t)$, $F_2(s,t)$ denote external longitudinal and transverse forces; whereas $M_1(s,t)$ denotes external in-plane moment.

Dynamical system (1)–(3) is characterized by the following properties: it is infinite-dimensional, and is composed of multi-fields that are coupled nonlinearly in an exact geometric manner. We are interested in deriving reduced order models for the dynamics of this coupled system. The reduced models will be used to relate proper orthogonal modes to normal modes of vibration. This could be done by a classical Galerkin projection onto a subspace spanned by linear normal modes of vibration. However, such a projection will not provide us with an optimal reduced order system. The term optimal refers to the least number of modes needed to capture a certain percentage of an appropriate energy like quantity of motion. An optimal reduced system is one that is based on the normal modes of vibration of the system.

Coupled dynamical system (1)–(3) should possess numerous normal modes of vibration at least for small energy levels since the linearized system and the reduced linearized systems, which are the linear rod and beam, possess well-defined normal modes of vibration. When light viscous dissipation is added, the forced system should possess attractors residing on low-dimensional invariant manifolds since invariant manifold of motion reflecting normal modes of vibration will continue to be invariant when dissipation is added [23]. So an attractor on an invariant manifold carries information on the spatial structure of the latter. It is shown in Georgiou [24] that this information can be elegantly extracted by a POD analysis of a segment of the trajectory of the attractor. In this work, we show that the POD modes of attractors or even transients in the vicinity of two-dimensional invariant manifolds provide reduced order models capable of reproducing the dynamics of the full order system for a wide range of forcing parameters.

To better understand the results of the POD analysis and the properties of the reduced order system, we should be aware of the fact that our coupled system possesses at least two categories of normal modes of vibration:

A normal mode of *synchronous vibrations* is characterized mathematically as follows:

$$(u_1(s,t), u_2(s,t), \theta_3(s,t)) = Q(t)(\varphi_1(s;E), \varphi_2(s;E), \varphi_3(s;E)), \tag{4}$$

where $Q(t)$ is the amplitude and $(\varphi_1(s;E), \varphi_2(s;E), \varphi_3(s;E))$ is the shape of the normal mode of vibration. The shape is a continuous function of the total mechanical energy E up to a certain energy level.

A normal mode *of no synchronous vibrations* is characterized mathematically as follows:

$$\left.\begin{aligned}&(u_1(s,t), u_2(s,t), \theta_3(s,t))\\ &\quad = (f(Q(t), \dot{Q}(t))\varphi_1(s;E),\ Q(t)\varphi_2(s;E),\ Q(t)\varphi_3(s;E))\end{aligned}\right\}. \tag{5}$$

In this normal mode of vibration, the axial displacement is slaved via a nonlinear relation (single-valued function) $f(Q(t), \dot{Q}(t))$ to the synchronized motion of transverse and rotational displacement fields, namely the amplitude of the axial field is a function of the common amplitude of the other two fields. This is a master-slaved normal mode of vibration and is realized as a two-dimensional invariant manifold in phase space. Coupled structural and mechanical systems composed of subsystems with low and high natural frequencies possess master-slaved type normal modes realized as global invariant manifolds in phase space. An example of such a system is a cantilever beam coupled to a pendulum [25] and a nonlinear plate [26].

For a nonlinear coupled system with multi-fields, such as the one we consider here, it is very hard or even impossible to compute analytically the normal modes of vibration. Here we derive reduced order models using POD modes to relate the latter to normal modes of vibration. We use the proper

orthogonal modes of a motion to derive optimal reduced order models for geometrically exact coupled models for rods. The POD modes of motions are extracted from the dynamics of a finite element model of a geometrically exact nonlinear rod. Georgiou and Schwartz [17] and Georgiou and coworkers [25] show that, under certain conditions, a motion characterized by a very small number (one or two) of POD modes resides near a two-dimensional invariant manifold associated to a normal mode of vibration. The physical meaning of POD modes for systems with low level of complexity in regards to dimensionality and coupling – for example, linear and nonlinear systems with single fields – has been addressed in works [16, 17]. In this work, we shall have the opportunity to assign physical meaning to POD modes of coupled systems with high level of complexity in regards to coupling of involved multi-fields.

3. Basics of POD Analysis of Multi-Field Structural Systems

We assume that we can compute the dynamics of the rod as precisely as desired. In particular, information on the dynamics is obtained by high performance algorithms based on the method of finite elements [14]. The computational dynamics are analyzed systematically by the method of proper orthogonal decomposition (POD) as it has been developed in Georgiou [15] to study multi-field dynamics of coupled nonlinear structural systems. The POD method characterizes the spatial structure of a motion in terms of proper orthogonal modes. These modes will be used to reduce the dimension of the coupled equations of motion.

We present a summary of the proper orthogonal decomposition technique for the dynamics of coupled structural systems whose physical domain is modeled as one-dimensional manifold embedded in three-dimensional Euclidean space. Such a system is a generic spatial rod. Here we mention that the POD development for coupled multi-fields in structural dynamics is based on the time and space auto-correlation operators, which are considered to be primitive quantities of motion. A detail development of the POD method for coupled structural dynamics is given in Georgiou [15], where a discrete version of the POD method is combined with the finite element method to systematically characterize coupled vibrations in generic nonlinear rods.

The multi-field dynamics of a planar rod are described mathematically by a vector field defined as follows:

$$\boldsymbol{V}(s,t) \equiv (u_1(s,t), u_2(s,t), \theta_3(s,t))^{\mathrm{T}}, \tag{6}$$

where $s \in [0, L]$ and $t \in (0, t_f < +\infty)$ are respectively space and time independent variables. Italic bold-faced majuscules denote vectors and matrices. The superscript T denotes the transpose of a vector or matrix. Vector field (6) describes the trajectory of a motion in the space of configurations.

We decompose the trajectory of a motion over a specified time interval into a set of proper orthogonal modes. These modes will be used to derive reduced order models. The novel feature of this POD analysis resides in the fact that information on the trajectory of a motion is obtained by means of finite element algorithms and not by analytic or semi-analytic methods lowering the complexity of the model, thus diminishing its predictability.

The trajectory of a motion over the interval of time $[T_1, T_2]$ can be characterized optimally by the time auto-correlation operator:

$$C(t,\tau) \equiv \frac{2}{L}\int_0^L \boldsymbol{V}(s,t)\cdot\boldsymbol{V}(s,\tau)ds, \quad t,\tau \in [T_1, T_2]. \tag{7}$$

The trace of operator (7) defines a positive definite quadratic quantity of the vector field:

$$E_C \equiv \frac{2}{T_2 - T_1} \int_{T_1}^{T_2} C(t,t)\, dt$$
$$= \frac{2}{T_2 - T_1} \int_{T_1}^{T_2} \left\{ \frac{2}{L} \int_0^L u_1^2(s,t) + u_2^2(s,t) + \theta_3^2(s,t)\, ds \right\} dt > 0. \tag{8}$$

It is called the auto-correlation energy. The time auto-correlation of the vector field defines a non-negative Hermitian (symmetric) operator [27], which in turn is used to define the following eigen-problem:

$$\frac{2}{T_2 - T_1} \int_{T_1}^{T_2} C(t,\tau) A_m(\tau)\, dt = \lambda_m A_m(t), \quad m = 1, \ldots, M < \infty. \tag{9}$$

This problem defines a sequence of eigen-numbers $\lambda_m > 0$ and a corresponding sequence of eigen-functions $A_m(t)$, amplitudes. Since the operator is symmetric, the amplitudes are orthonormal:

$$\frac{2}{T_2 - T_1} \int_{T_1}^{T_2} A_m(t) A_n(t)\, dt = \delta_{mn}, \tag{10}$$

where δ_{mn} is the Kronecker delta symbol. Since the sum of the eigen-numbers gives the trace of the operator, which by definition is the auto-correlation energy (8), an eigen-value represents a fraction of the auto-correlation energy. Indeed, we have the relation:

$$E_C = \sum_{m=1}^{\infty} \lambda_m > 0. \tag{11}$$

The projection of the evolution of the vector field over the time interval $[T_1,\ T_2]$, namely the trajectory of the motion, onto the amplitude $A_m(t)$ defines the following vector-valued function (shape) over the space domain $[0,\ L]$:

$$\boldsymbol{\Phi}_m(s) \equiv \frac{2}{T_2 - T_1} \int_{T_1}^{T_2} A_m(t) \boldsymbol{V}(s,t)\, dt. \tag{12}$$

It can be shown that shapes (12) form an orthogonal set of functions in the sense that

$$\langle \boldsymbol{\Phi}_m(s), \boldsymbol{\Phi}_n(s) \rangle \equiv \sqrt{\frac{2}{L} \int_0^L \boldsymbol{\Phi}_m(s) \cdot \boldsymbol{\Phi}_n(s) ds} = \sqrt{\lambda_m} \sqrt{\lambda_n} \delta_{mn}. \tag{13}$$

The above defined sequences: the auto-correlation energy fractions $\{\lambda_m\}_{m=1}^M$ – called the POD energy spectrum, their companion amplitudes $\{A_m(t)\}_{m=1}^M$, and their companion shapes $\{\boldsymbol{\Phi}_m(s)\}_{m=1}^M$ characterize uniquely and optimally the trajectory of a motion. In fact, it can be shown that these sequences infer the following optimal decomposition of the trajectory of the motion:

$$\boldsymbol{V}(s,t) = \sum_{m=1}^{\infty} Q_m(t) \boldsymbol{\Psi}_m(s), \tag{14}$$

where the amplitudes and shapes are given by

$$Q_m(t) \equiv A_m(t)\sqrt{\lambda_m}, \quad \sqrt{\lambda_m}\boldsymbol{\Psi}_m(s) \equiv \Phi_m(s). \tag{15}$$

Expansion (14) is called a proper orthogonal decomposition of the vector field describing the trajectory of the motion of the coupled system. Decomposition (14) will be used to determine the governing degrees-of-freedom, called POD modes, of the complicated coupled equations of motion (1)–(3). These modes will be used to reduced the dimension coupled system (1)–(3), called the full-order system.

3.1. Characterization of Coupling

Given a dynamical system with coupled multi-fields, one of the basic issues is to determine the strength of coupling among its constituent fields. The field coupling during a motion can be quantified by the norms of the components of the POD modes. The shape of the mth POD mode of a motion of the planar rod is described by the vector-valued function,

$$\begin{aligned}\boldsymbol{\Psi}_m(s) &\equiv (\Psi_{1m}(s), \Psi_{2m}(s), \Psi_{3m}(s))^{\mathrm{T}} \\ &= (C_{1m}\psi_{1m}(s), C_{2m}\psi_{2m}(s), C_{3m}\psi_{3m}(s))^{\mathrm{T}}.\end{aligned} \tag{16}$$

In Equation (16), we have introduced the normalized shapes for the components of the mode:

$$\langle \psi_{km}(s), \psi_{kn}(s)\rangle \equiv \sqrt{\frac{2}{L}\int_0^L \psi_{km}(s)\psi_{kn}(s)ds} = 1, \quad k = 1, 2, 3. \tag{17}$$

Moreover, the constants C_{km} denote the norms of the components of the mode:

$$C_{km} \equiv \langle \Psi_{km}(s), \Psi_{km}(s)\rangle \equiv \sqrt{\frac{2}{L}\int_0^L \Psi_{km}(s)\Psi_{km}(s)ds}, \quad k = 1, 2, 3. \tag{18}$$

Since the POD modes are orthonormal by construction, the norms of the components of a POD mode satisfy the relation:

$$C_{1m}^2 + C_{2m}^2 + C_{3m}^2 = 1. \tag{19}$$

Normalized shapes (17) and corresponding norms (18) are computed by properly processing the discrete version of a POD mode, obtained by a POD analysis of the finite element dynamics [12]. Clearly the norms C_{km} define the strength of coupling among the three fields for the dynamics of the planar rod. This is particularly useful for motions that are dominated by a small number of POD modes. Indeed, numerical experiments reveal a plethora of motions, free and forced, dominated by a single POD mode. We concentrate on the POD analysis and computation of reduced models for these motions. As we shall see, these motions, under certain conditions, belong to a family of motions forming a certain normal mode of vibration.

Table 1. Properties of the planar rod whose dynamics is approximated by a finite element model for geometrically exact rods.

Length (L)	10.00
Area (A)	1.00
Modulus of elasticity in extension (E)	12000.00
Modulus of elasticity in shearing (G)	5000.00
Material density (ρ)	$1.00E-06$
Viscous dissipation (D)	$5.00E-04$

Figure 1. Schematic diagram of a pinned-pinned planar rod. The dynamics is computed by the method of finite elements.

3.2. Some Results of the POD Analysis for the Exact Rod

We analyze by means of the POD technique various free and forced motions of the planar rod depicted in Figure 1. The rod is excited by an external transverse load that is spatially uniform and time varying. Table 1 gives the geometric and material properties of the rod. All quantities have consistent units. The ratio of thickness to length is 0.10. Thus, we have a moderately thick rod. We expect weak modal interactions for motions close to the first and second normal modes. Modal interactions will increase as the order of normal mode increases. The normal modes of vibration are not known. In this work, we shall show how POD analysis of a finite element model can identify some normal modes of vibration.

POD analysis of numerical experiments reveal that there exist a plethora of motions of the rod, either free or forced, dominated by a single POD mode, namely the auto-correlation energy is concentrated at a single POD mode; whereas, a tiny fraction of the energy is spread over 3–5 modes. Figure 2 shows the POD spectrum of the long time trajectory of a forced motion. Notice that the dominant POD mode contains more than 99.98% of the auto-correlation energy. The eigen-values (energy fractions) are normalized with respect to total auto-correlation energy.

One interesting result is the fact that the response of the rod to the harmonic forcing is characterized by a very small number of dominant POD modes. In fact, for relatively small to moderate level of forcing amplitude, the forced vibrations of the rod are dominated by a single POD mode. This happens

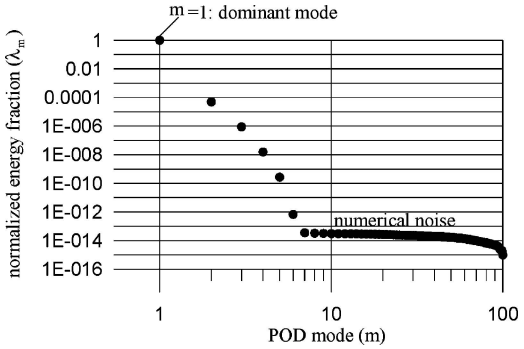

Figure 2. Typical POD spectrum of a motion dominated by a single POD mode.

Table 2. Ordered natural frequencies (rad/s) of the linear rod and beam: used as approximate natural frequencies to numerate the unknown normal modes of vibration of the nonlinear rod.

rad/sec	rad/sec	rad/sec
$\omega_1 = \omega_1^b = 3121.043$	$\omega_6 = \omega_2^r = 68828.85$	$\omega_{11} = \omega_7^b = 157931.10$
$\omega_2 = \omega_2^b = 12484.17$	$\omega_7 = \omega_5^b = 78026.07$	$\omega_{12} = \omega_5^r = 172072.11$
$\omega_3 = \omega_3^b = 28089.39$	$\omega_8 = \omega_3^r = 103243.27$	$\omega_{13} = \omega_8^b = 199747.75$
$\omega_4 = \omega_1^r = 34414.42$	$\omega_9 = \omega_6^b = 112357.55$	$\omega_{14} = \omega_6^r = 206486.54$
$\omega_5 = \omega_4^b = 49936.69$	$\omega_{10} = \omega_4^r = 137657.69$	$\omega_{15} = \omega_9^b = 252804.48$

when the forcing frequency is close to a natural frequency of the rod. Under certain conditions we can approximate the natural frequencies with those of the linearized system: For vanishing shearing, a condition satisfied for thin rods, the system could be reduced to an uncoupled system that consists of the classical linear rod for the longitudinal motions and the classical linear beam for the transverse motions. Table 2 orders in increasing values the frequencies of the uncoupled rod and beam reduced systems. These frequencies guide us to determine frequencies of harmonic forcing that give rise to motions characterized by a single POD mode.

We present the shapes of the POD modes for steady-state forced vibrations (attractors) excited by harmonic forcing at frequencies close to the natural frequencies of the first and third modes of the linear beam (Table 1). The POD modes of these motions will be used to derive reduced order models for the dynamics of the full order system (1)–(3). Excitation at low frequency and around the first natural frequency of the linear beam reveals that the auto-correlation energy is almost contained in three POD modes. *However, a single POD mode dominates* the motion. Table 3 gives the energies and norms of the components of the first three POD modes for the attractor of a forced vibration at low frequency. Figure 3 gives the normalized shapes of these three POD modes. Table 3 and Figure 4 give the POD characterization of a forced vibration due to harmonic forcing at frequency close to the third natural frequency of the linear beam. The important feature for these motions is the fact that their auto-correlation energy is contained almost at a single mode. Such motions have the lowest possible dimensional complexity and therefore we should attempt to determine whether they belong to a normal mode of vibration.

Clearly a motion dominated by a single POD mode can be represented as follows:

$$\boldsymbol{V}(s,t) \cong \boldsymbol{V}_3(s,t) \equiv Q_1(t)\boldsymbol{\Psi}_1(s) + Q_2(t)\boldsymbol{\Psi}_2(s) + Q_3(t)\boldsymbol{\Psi}_3(s). \tag{20}$$

The above 3-POD mode representation contains almost the whole amount of the auto-correlation energy since $\lambda_1 + \lambda_2 + \lambda_3 = 0.9998 + O(10^{-3})$. The remarkable result is the fact that a single mode dominates

Table 3. POD characterization of a forced vibration of the planar rod at frequency close to the first natural frequency of the linear beam.

POD mode k	Energy (λ_k)	Axial (C_{k1})	Transverse (C_{k2})	Rotatory (C_{k3})
1	0.999949	$3.411668E-005$	0.955834	0.293908
2	$4.948872E-05$	0.9999993	$8.843624E-004$	$7.76783E-004$
3	$8.795890E-07$	$1.221165E-003$	0.7830365	0.62197

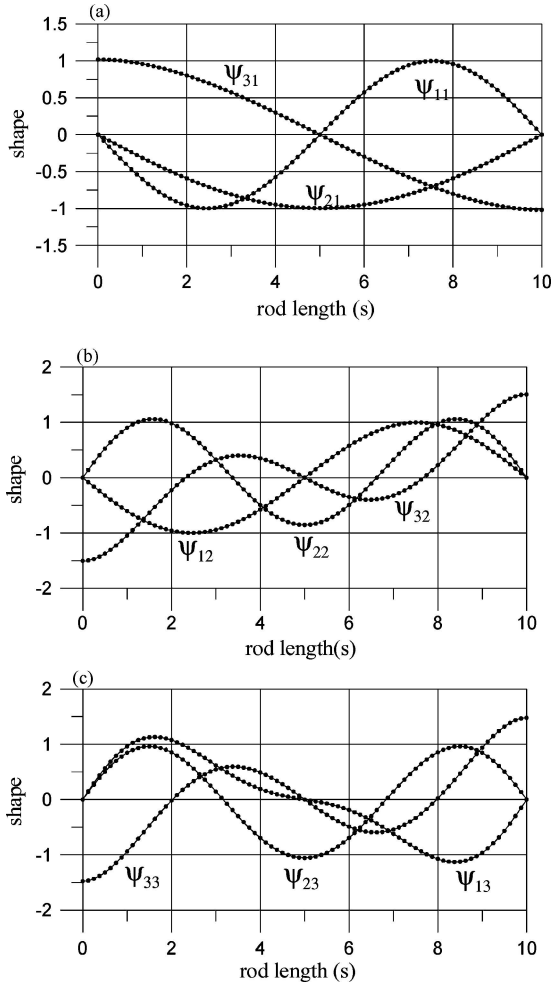

Figure 3. The normalized shapes of the components of the (a) first, (b) second and (c) third POD modes of a forced vibration of the planar rod at forcing frequency close to the first natural frequency of the linear beam.

the motions. Regarding the inter-modal coupling in the dominant POD mode, the level of coupling of the axial component to the transverse and rotation component is very weak; whereas, the coupling between the transverse and the rotational component is strong (Tables 3 and 4). This POD quantification of the coupling strength among the various fields seems to provide a potential tool for a systematic characterization of vibrations in structural system with multi-field dynamics.

The above result forms the impetus to derive reduced order models using at least three POD modes. We conjecture that the POD analysis of the trajectory of the attractor of a motion characterizes the spatial

Table 4. POD characterization of a forced vibration of the planar rod at frequency close to the third natural frequency of the linear beam.

POD mode k	Energy (λ_k)	Axial (C_{k1})	Transverse (C_{k2})	Rotatory (C_{k3})
1	0.998933	$1.232707E-006$	0.808839	0.5880292
2	$1.066845E-03$	$1.64421E-004$	0.928430	0.3715070
3	$1.367602E-07$	0.999999	$2.272344E-004$	$1.779860E-004$

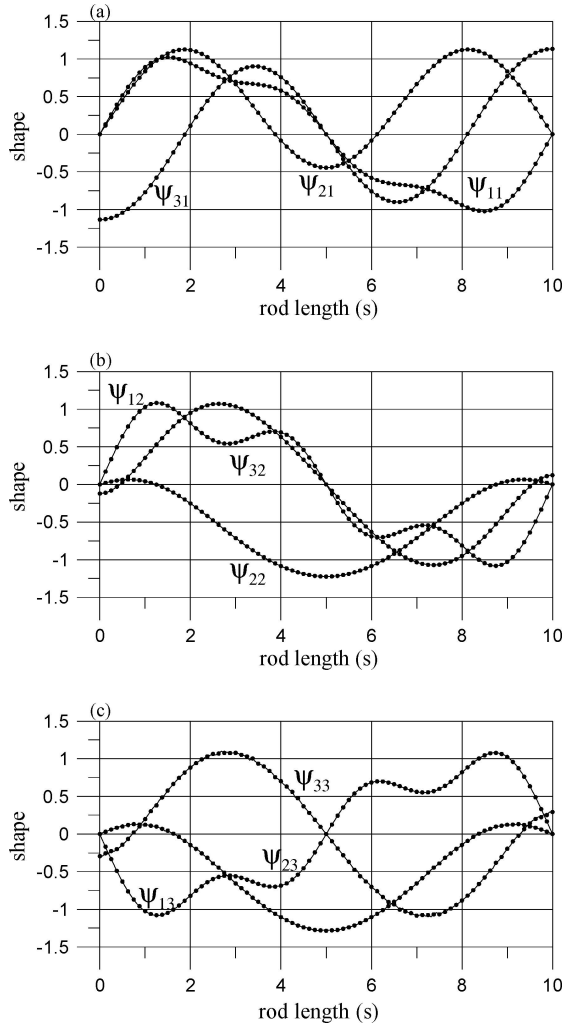

Figure 4. The normalized shapes of the components of the (a) first, (b) second and (c) third POD modes of a forced vibration of the planar rod at forcing frequency close to the third natural frequency of the linear beam.

structure of the invariant subspace that carries the attractor [24]. The derived reduced model can be used to determine whether the generalized (principal) coordinates furnished by the POD modes parameterize adequately an invariant manifold. Here of interest are two-dimensional invariant manifolds because they could represent normal modes of vibration.

Remark: Since the dynamics is dominated by a single POD mode, we could have attempted to retain only the dominant POD mode in truncation (20). This, however, could not be an adequate representation due to the fact that nonlinearity interacts with dissipation at low levels of energy and the possibility that the dominant POD mode slaves some of the other modes.

4. POD Reduced Order Models

In this section we derive reduced order systems by directly projecting the full order system, the complicated coupled equations of motion for the planar rod, onto a specified set of POD modes. The motion

is represented by a vector-valued function, which we rewrite,

$$\begin{aligned}\boldsymbol{V}(s,t) &\equiv (V_1(s,t),\, V_2(s,t),\, V_3(s,t))^{\mathrm{T}} \\ &\equiv (u_1(s,t),\, u_2(s,t),\, \theta_3(s,t))^{\mathrm{T}}.\end{aligned} \tag{21}$$

We write the equations of motion in a compact form to perform various projection operations efficiently. To this end, we linearize the equations of motion about the reference configuration (zero solution) to get

$$\left.\begin{aligned}&\rho A\frac{\partial^2 u_1(s,t)}{\partial t^2} + D\frac{\partial u_1(s,t)}{\partial t} - EA\frac{\partial^2 u_1(s,t)}{\partial s^2} = F_1(s,t). \\ &\rho A\frac{\partial^2 u_2(s,t)}{\partial t^2} + D\frac{\partial u_2(s,t)}{\partial t} - GA\left(\frac{\partial^2 u_2(s,t)}{\partial s^2} - \frac{\partial \theta_3(s,t)}{\partial s}\right) = F_2(s,t) \\ &\rho I\frac{\partial^2 \theta_3(s,t)}{\partial t^2} + D\frac{\partial \theta_3(s,t)}{\partial t} - EI\frac{\partial^2 \theta_3(s,t)}{\partial s^2} \\ &\quad - GA\left(\frac{\partial u_2(s,t)}{\partial s} - \theta_3(s,t)\right) = M_1(s,t).\end{aligned}\right\} \tag{22}$$

Equations (22) are the well-known Timoshenko beam equations of motion [21]. In view of linearized system (22), we define the *inertia* and *dissipation* linear operators:

$$\boldsymbol{L}_M[\boldsymbol{V}] \equiv \left[\rho A\frac{\partial^2 u_1}{\partial t^2},\, \rho A\frac{\partial^2 u_2}{\partial t^2},\, \rho I\frac{\partial^2 \theta_3}{\partial t^2}\right]^{\mathrm{T}}, \tag{23}$$

$$\boldsymbol{L}_D[\boldsymbol{V}] \equiv \left[D\frac{\partial u_1}{\partial t},\, D\frac{\partial u_2}{\partial t},\, D\frac{\partial \theta_3}{\partial t}\right]^{\mathrm{T}}. \tag{24}$$

In view of definitions (23) and (24), the original equations of motion assume the following compact form:

$$\boldsymbol{L}_M[\boldsymbol{V}(s,t)] + \boldsymbol{L}_D[\boldsymbol{V}(s,t)] + \boldsymbol{L}_{EL}[\boldsymbol{V}(s,t)] = \boldsymbol{F}(s,t), \tag{25}$$

where $\boldsymbol{L}_{LE}[\boldsymbol{V}(s,t)]$ is a nonlinear operator, given in appendix, and term

$$\boldsymbol{F}(s,t) \equiv (F_1(s,t),\ F_2(s,t),\ M_1(s,t))^{\mathrm{T}} \tag{26}$$

designates a forcing term.

To bring out the full linear structure of the equations of motion, we introduce the linear *stiffness* operator,

$$\boldsymbol{L}_K[\boldsymbol{V}] \equiv \left[-AE\frac{\partial^2 u_1}{\partial s^2}, -GA\left(\frac{\partial^2 u_2}{\partial s^2} - \frac{\partial \theta_3}{\partial s}\right), -EI\frac{\partial^2 \theta_3}{\partial s^2} - GA\left(\frac{\partial u_2}{\partial s} - \theta_3\right)\right]^{\mathrm{T}}, \tag{27}$$

and the *pure nonlinearity* operator,

$$\boldsymbol{L}_{NL}[\boldsymbol{V}(s,t)] \equiv \boldsymbol{L}_{EL}[\boldsymbol{V}(s,t)] - \boldsymbol{L}_K[\boldsymbol{V}(s,t)]. \tag{28}$$

In view of the above-defined operators, original dynamical system (1)–(3) assumes the following compact form:

$$\left.\begin{aligned} \boldsymbol{L}[\boldsymbol{V}(s,t)] \equiv \underbrace{\boldsymbol{L}_M[\boldsymbol{V}(s,t)] + \boldsymbol{L}_D[\boldsymbol{V}(s,t)] + \boldsymbol{L}_K[\boldsymbol{V}(s,t)]}_{\text{Linear}} \\ + \boldsymbol{L}_{NL}[\boldsymbol{V}(s,t)] = \boldsymbol{F}(s,t) \end{aligned}\right\}. \tag{29}$$

Formulation (29) is generic; it can be applied to derive compact formulations for the equations of motion of geometrically exact models for spatial rods and shells.

4.1. The Galerkin Projection

Now we derive reduced order systems by projecting the full order system onto a function space spanned by a specified number of POD modes. To this end, we truncate the motion $\boldsymbol{V}(s,t)$ at M POD modes:

$$\boldsymbol{V}_M(s,t) \equiv \sum_{m=1}^{M} Q_m(t)\boldsymbol{\Psi}_m(s) = \boldsymbol{\Psi}(s)\boldsymbol{Q}(t). \tag{30}$$

The $M \times 1$ vector $\boldsymbol{Q}(t)$ denotes the amplitudes of the POD modes; whereas the columns of the $3 \times M$ matrix-valued function $\boldsymbol{\Psi}$ coincide with the shapes of the POD modes. Because of the optimality of the POD data process, vector $\boldsymbol{Q}(t)$ designates principal directions identified to the ones furnished by the natural basis for the M-dimensional vector space.

The order of truncation is based on the criterion that the selected M modes contain a certain fraction of the auto-correlation energy, that is,

$$\sum_{m=1}^{M} \lambda_m \leq \alpha E_C, \ 0 < \alpha \leq 1. \tag{31}$$

For the specific class of motions of the planar rod that we are interested, the criterion is $\alpha \simeq 0.9998$ for $M = 3$ POD modes.

Upon projecting the equations of motion (1)–(3) onto the function space spanned by the M POD modes, we get the following equation:

$$\left.\begin{aligned} &\langle \boldsymbol{L}[\boldsymbol{V}_M(s,t)], \boldsymbol{\Psi}_m(s)\rangle \equiv \frac{2}{L}\int_0^L \boldsymbol{L}[\boldsymbol{V}_M(s,t)] \cdot \boldsymbol{\Psi}_m(s) ds \\ &= \frac{2}{L}\int_0^L (\boldsymbol{L}_M[\boldsymbol{V}_N(s,t)] \cdot \boldsymbol{\Psi}_m(s) + \boldsymbol{L}_D[\boldsymbol{V}_M(s,t)] \cdot \boldsymbol{\Psi}_m(s) + \boldsymbol{L}_K[\boldsymbol{V}_M(s,t)] \cdot \boldsymbol{\Psi}_m(s)) ds \\ &\quad + \frac{2}{L}\int_0^L \boldsymbol{L}_{NL}[V_M(s,t)] \cdot \boldsymbol{\Psi}_m(s) ds \\ &= \langle \boldsymbol{F}(s,t), \boldsymbol{\Psi}_m(s)\rangle \equiv \frac{2}{L}\int_0^L \boldsymbol{F}(s,t) \cdot \boldsymbol{\Psi}_m(s) ds. \end{aligned}\right\} \tag{32}$$

After carrying out the projections in Equation (32), we obtain the following compact equation for the reduced order system:

$$\boldsymbol{M}\ddot{\boldsymbol{Q}}(t) + \boldsymbol{D}\dot{\boldsymbol{Q}}(t) + \boldsymbol{K}\boldsymbol{Q}(t) + \underbrace{\frac{2}{L}\int_0^L \boldsymbol{N}(\boldsymbol{\Psi}(s)\boldsymbol{Q}(t)) ds}_{\text{integral nonlinearity}} = \boldsymbol{f}(t). \tag{33}$$

In Equation (33) the fourth term designates a nonlinearity, *which is of integral type due to the exact modeling of the geometric nonlinearity*. It is a very complicated mathematical expression composed of trigonometric functions of the rotation field, see appendix.

The $M \times M$ matrices: $\boldsymbol{M}$, $\boldsymbol{D}$, $\boldsymbol{K}$ denote the effective mass, dissipation, and stiffness properties of the reduced order system. They are given by the following closed form expressions obtained elegantly by means of symbolic computations (code MAPLE). The elements of the mass, dissipation, and stiffness matrices are respectively given by

$$\begin{aligned} M_{nm} &= \langle \boldsymbol{L}_M(\boldsymbol{\Psi}_n), \boldsymbol{\Psi}_m \rangle = M_{mn} = \langle \boldsymbol{L}_M(\boldsymbol{\Psi}_m), \boldsymbol{\Psi}_n \rangle \\ &= \rho A C_{1n} C_{1m} \langle \psi_{1n}, \psi_{1m} \rangle + \rho A C_{2n} C_{2m} \langle \psi_{2n}, \psi_{2m} \rangle \\ &\quad + \rho I C_{3n} C_{3m} \langle \psi_{3n}, \psi_{3m} \rangle, \end{aligned} \tag{34}$$

$$\begin{aligned} D_{nm} &\equiv \langle \boldsymbol{L}_D(\boldsymbol{\Psi}_n), \boldsymbol{\Psi}_m \rangle = D_{mn} = \langle \boldsymbol{L}_D(\boldsymbol{\Psi}_m), \boldsymbol{\Psi}_n \rangle \\ &= D C_{1n} C_{1m} \langle \psi_{1n}, \psi_{1m} \rangle + D C_{2n} C_{2m} \langle \psi_{2n}, \psi_{2m} \rangle + D C_{3n} C_{3m} \langle \psi_{3n}, \psi_{3m} \rangle, \end{aligned} \tag{35}$$

$$\begin{aligned} K_{nm} &\equiv \langle \boldsymbol{L}_K(\boldsymbol{\Psi}_n), \boldsymbol{\Psi}_m \rangle \\ &= -C_{1n} C_{1m} A E \langle \psi_{1n}, \psi_{1m,ss} \rangle - C_{2n} C_{2m} A G \langle \psi_{2n}, \psi_{2m,ss} \rangle \\ &\quad - C_{3n} C_{3m} E I \langle \psi_{3n}, \psi_{3m,ss} \rangle \\ &\quad \underbrace{- C_{3n} C_{2m} A G \langle \psi_{3n}, \psi_{2m,s} \rangle + C_{2n} C_{3m} A G \langle \psi_{2n}, \psi_{3m,s} \rangle}_{\text{coupling}} \\ &\quad + C_{3n} C_{3m} A G \langle \psi_{3n}, \psi_{3m} \rangle, \end{aligned} \tag{36}$$

$$\begin{aligned} K_{mn} &\equiv \langle \boldsymbol{L}_K(\boldsymbol{\Psi}_m), \boldsymbol{\Psi}_n \rangle \\ &= -C_{1m} C_{1n} A E \langle \psi_{1m}, \psi_{1n,ss} \rangle - C_{2m} C_{2n} A G \langle \psi_{2m}, \psi_{2n,ss} \rangle \\ &\quad - C_{3m} C_{3n} E I \langle \psi_{3m}, \psi_{3n,ss} \rangle \\ &\quad \underbrace{- C_{3m} C_{2n} A G \langle \psi_{3m}, \psi_{2n,s} \rangle + C_{2m} C_{3n} A G \langle \psi_{2m}, \psi_{3n,s} \rangle}_{\text{coupling}} \\ &\quad + C_{3m} C_{3n} A G \langle \psi_{3m}, \psi_{3n} \rangle. \end{aligned} \tag{37}$$

4.2. Properties

The closed form expressions for the mass, dissipation, and stiffness matrices show that any two POD modes interact at the linearity level even though they are orthogonal by construction. It is necessary to consider the properties of these matrices.

Property 1: The mass, dissipation, and stiffness matrices are not diagonal even though the POD modes designate principal directions. So we have cross coupling among the POD modes even though they are orthogonal. This coupling is due to the fact that the individual components of a POD mode are not orthogonal to the corresponding components of another POD mode. Clearly this is a property of multi-field coupled dynamical systems.

Property 2: Regarding the structure of the stiffness matrix, we notice in the diagonal elements a coupling between the transverse and rotatory components of a POD mode. This coupling quantifies the effect of shearing on the linear natural frequencies of the full order system. This effect appears also in the off-diagonal terms revealing a shearing cross coupling of the two different POD modes.

Property 3: While it is easy to deduce the symmetry properties for the mass and dissipation matrices, the same cannot be concluded for the stiffness matrix *without prior knowledge of the shapes of the POD modes*. The stiffness matrix should be symmetric: $\boldsymbol{K}^{\mathrm{T}} = \boldsymbol{K}$. In fact, this property can be used as a diagnostic tool to verify whether the POD modes have been computed correctly and processed properly to extract the norms and normalized shapes of the components.

Property 4: We claim that the mass, dissipation, and stiffness matrices ought to be positive definite, namely,

$$v \cdot \boldsymbol{M} v > 0, v \cdot \boldsymbol{D} v > 0, v \cdot \boldsymbol{K} v > 0, \tag{38}$$

where v denotes an arbitrary element of the M-dimensional vector space [28]. This is because these properties characterize the linearized system and must be invariant in regards to a change of the coordinate system, such as the one furnished by the POD modes. Therefore, the structure of the POD modes should be such as to render these matrices positive definite. We will verify the above properties by directly computing the matrices for several free and forced motions once we have computed their POD modes.

5. The 3-DOF Reduced System

For the category of motions dominated by a single POD, we truncate the reduced order system at three degrees-of-freedom (3-DOF). Truncation to include only the dominant POD mode is not recommended since we have linear mass, dissipation, and elasticity coupling between any two POD modes. Truncation at 3-DOF contains more that 99.98% of the auto-correlation energy. The following amplitude equations describe the 3-DOF reduced system:

$$\left.\begin{aligned}
&\begin{pmatrix} M_{11} & M_{12} & M_{13} \\ M_{21} & M_{22} & M_{23} \\ M_{31} & M_{32} & M_{33} \end{pmatrix} \begin{pmatrix} \ddot{Q}_1(t) \\ \ddot{Q}_2(t) \\ \ddot{Q}_3(t) \end{pmatrix} + \begin{pmatrix} D_{11} & D_{12} & D_{13} \\ D_{21} & D_{22} & D_{23} \\ D_{31} & D_{32} & D_{33} \end{pmatrix} \begin{pmatrix} \dot{Q}_1(t) \\ \dot{Q}_2(t) \\ \dot{Q}_3(t) \end{pmatrix} \\
&+ \begin{pmatrix} K_{11} & K_{12} & K_{13} \\ K_{21} & K_{22} & K_{23} \\ K_{31} & K_{32} & K_{33} \end{pmatrix} \begin{pmatrix} Q_1(t) \\ Q_2(t) \\ Q_3(t) \end{pmatrix} + \frac{2}{L} \begin{pmatrix} \displaystyle\int_0^L N_1 \left(\sum_{m=1}^{3} Q_m(t) \boldsymbol{\Psi}_m(s) \right) ds \\ \displaystyle\int_0^L N_2 \left(\sum_{m=1}^{3} Q_m(t) \boldsymbol{\Psi}_m(s) \right) ds \\ \displaystyle\int_0^L N_3 \left(\sum_{m=1}^{3} Q_m(t) \boldsymbol{\Psi}_m(s) \right) ds \end{pmatrix} = \begin{pmatrix} f_1(t) \\ f_2(t) \\ f_3(t) \end{pmatrix}
\end{aligned}\right\}. \tag{39}$$

For the case of transverse external forcing which is spatially uniform and varying harmonically in time, $F_2(s,t) = P\cos(\Omega t)$, the POD-modal forces in the right hand side of system (39) assume the following expressions:

$$\begin{aligned}
f_1(t) &= \langle \boldsymbol{F}(s,t), \boldsymbol{\Psi}_1(s) \rangle = \frac{2PC_{21}}{L} \int_0^L \psi_{21}(s)\, ds \times \cos(\Omega t), \\
f_2(t) &= \langle \boldsymbol{F}(s,t), \boldsymbol{\Psi}_2(s) \rangle = \frac{2PC_{22}}{L} \int_0^L \psi_{22}(s)\, ds \times \cos(\Omega t), \\
f_3(t) &= \langle \boldsymbol{F}(s,t), \boldsymbol{\Psi}_3(s) \rangle = \frac{2PC_{23}}{L} \int_0^L \psi_{23}(s)\, ds \times \cos(\Omega t).
\end{aligned} \tag{40}$$

The dynamics of reduced system (39) is computed numerically. Integration over a time interval of interest is carried out by the fourth order Runge–Kutta method. For a given time instance, system (39) is integrated exactly over the physical domain of the rod by means of the Legendre–Gauss integration scheme.

6. The POD-Reduced Model Method

The components of the POD modes appear in the mass, dissipation, and stiffness matrices. So these matrices should contain information on the dynamics of the full order system. For instance, such information is natural frequencies and damping factors. Therefore, we analyze the 3-DOF reduced system by performing an eigen-value analysis of its linearization to compute in particular the natural frequencies and companion shapes of the normal modes.

Let $\{\omega_m\}_{m=1}^{m=3}$ denote the linear natural frequencies of 3-DOF reduced system. They are the roots of the well-known characteristic polynomial,

$$\det\left(\boldsymbol{K} - \omega_m^2 \boldsymbol{M}\right) = 0. \tag{41}$$

Let $\{\hat{\boldsymbol{E}}_m\}_{m=1}^{m=3}$ denote the companion eigen-vectors. They are the solutions to the following well-known matrix equation:

$$\left[\boldsymbol{K} - \omega_m^2 \boldsymbol{M}\right]\hat{\boldsymbol{E}}_m = \boldsymbol{0}. \tag{42}$$

We define the eigen-vector matrix,

$$\hat{\boldsymbol{E}} \equiv [\hat{\boldsymbol{E}}_1 \mid \hat{\boldsymbol{E}}_2 \mid \hat{\boldsymbol{E}}_3]. \tag{43}$$

We will compare it with the identity matrix,

$$\hat{\boldsymbol{I}} \equiv [\hat{e}_1 \mid \hat{e}_2 \mid \hat{e}_3], \tag{44}$$

where $\{\hat{e}_m\}_{m=1}^{m=3}$ is the natural basis of the three-dimensional vector space.

A segment of the trajectory of a given motion is characterized uniquely by the linear modes of the reduced system. The natural frequencies of the linearized reduced system will be referred to as the reduced model (RM)-frequencies and the companion eigen-vectors will be referred to as the RM-normal modes.

The POD analysis of a motion along with the modal analysis of the linearized reduced order system will be referred to as the proper orthogonal decomposition-reduced model (POD-RM) method.

7. On the Properties of the Mass, Dissipation, and Stiffness Matrices

To determine the properties of the above matrices, we perform a POD-RM analysis of several free motions of the planar rod, the full order system. The motions are approximated by the finite element method. To this end, we excite free dynamics by applying the following transverse load:

$$F_2(s, t) = P\, g(t), \tag{45}$$

where P is its spatially uniform magnitude and $g(t)$ defines its time distribution according to the expression:

$$\left.\begin{aligned} g(t) &= \frac{1}{\tau_0}, \quad 0 \le t < \tau_0 \\ g(t) &= 1, \quad \tau_0 \le t < 2\tau_0 \\ g(t) &= 0, \quad 2\tau_0 \le t \end{aligned}\right\}. \tag{46}$$

We take the above load to be of impulsive type by taking $2\tau_0 \ll \tau_1$, where $\tau_1 \simeq 0.002013$ s is the period corresponding to the fundamental frequency of the linear beam, which is at $\omega_1^b \simeq 3121.00$ rad/s. For the 3-DOF reduced system, the above impulsive load delivers the following effective initial velocities:

$$Q_m(t=0) \simeq \frac{I_m}{M_{mm}}, \quad m = 1, 2, 3, \tag{47}$$

where the terms I_m, $m = 1, 2, 3$, denote the effective impulses of the modal forces given by the expressions:

$$\left.\begin{aligned} I_m &\equiv \int_0^{2\tau_0} \langle \boldsymbol{F}(s,t), \Psi_m(s) \rangle \, dt = \int_0^{2\tau_0} f_m(s,t)\, dt \\ &= \int_0^{2\tau_0} P\, g(t) \left\{ \frac{2}{L} \int_0^L C_{2m} \psi_{2m}(s)\, ds \right\} dt = \frac{3 C_{2m} P \tau_0}{L} \int_0^L \psi_{2m}(s)\, ds. \end{aligned}\right\} \tag{48}$$

POD-RM analysis of a free motion: The free dynamics of the full order system are excited by an impulsive load, Equation (45), at magnitude $P = 1$, and time duration $\tau_0 = 2.50 \times 10^{-5}$. The finite element dynamics, with sufficiently high spatial and temporal resolution, are processed by the POD method to find that a single mode dominates the motion. Figure 5 depicts the shapes of the normalized components of the dominant POD mode. The numerical values of the mass, dissipation, and stiffness matrices of the 3-DOF reduced system are:

$$\begin{aligned} \boldsymbol{M} &= \begin{pmatrix} M_{11} & M_{12} & M_{13} \\ M_{21} & M_{22} & M_{23} \\ M_{31} & M_{32} & M_{33} \end{pmatrix} = \begin{pmatrix} 9.205609 & 0.084584 & 0.096631 \\ 0.084584 & 6.393570 & -0.144513 \\ 0.096631 & -0.144513 & 5.027159 \end{pmatrix} \times 10^{-7}, \\ \boldsymbol{D} &= \begin{pmatrix} D_{11} & D_{12} & D_{13} \\ D_{21} & D_{22} & D_{23} \\ D_{31} & D_{32} & D_{33} \end{pmatrix} = \begin{pmatrix} 5.000000 & 0.046041 & 0.053094 \\ 0.046041 & 5.000000 & -0.112761 \\ 0.053094 & -0.112761 & 5.000000 \end{pmatrix} \times 10^{-4}, \\ \boldsymbol{K} &= \begin{pmatrix} K_{11} & K_{12} & K_{13} \\ K_{21} & K_{22} & K_{23} \\ K_{31} & K_{32} & K_{33} \end{pmatrix} = \begin{pmatrix} 0.008724 & 0.000091 & 0.000099 \\ 0.000091 & 0.406442 & -0.00708 \\ 0.000099 & -0.00708 & 1.868279 \end{pmatrix} \times 10^{3}. \end{aligned} \tag{49}$$

The stiffness matrix turns out to be symmetric, a fact not known in advance, but conjectured on physical grounds. Notice the negative cross coupling in all matrices. An eigen-value analysis reveals that all matrices (49) are positive definite. This established property verifies the fact that the POD modes have been computed correctly and processed properly to extract the norms of their components as well as their normalized shapes.

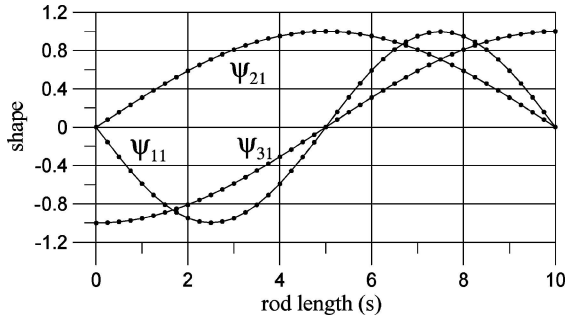

Figure 5. The normalized components of the dominant POD mode for the free dynamics of the rod excited by an impulsive transverse force.

The mass and stiffness matrices should contain information regarding the linearized natural frequencies of the full order system. The values for the linear natural frequencies (rad/s) of the 3-DOF reduced are

$$\omega_1 = 3078.549,\ \omega_2 = 25214.605,\ \omega_3 = 60986.457. \tag{50}$$

Indeed, it turns out that these frequencies are very close to the frequencies of the amplitudes of the three POD modes used for the reduction. More precisely, the amplitudes of the three POD modes have single frequencies respectively at 3067.21 rad/s, 25764.58 rad/s, and at 62571.12 rad/s. Moreover, numerical integration of the 3-DOF reduced system (39) with initial velocities given by relation (47) gives amplitudes with single frequencies very close to RM-frequencies (50). *So the reduced order system (derived from the free dynamics) contains frequency information of the full order system. This information on frequencies is contained in the shapes of the POD modes.*

The fact that the POD amplitudes have single frequencies is also reflected in the structure of the eigen-value matrix of the reduced system. For the above example, the numerical value of this matrix is

$$\hat{\boldsymbol{E}} \equiv [\hat{\boldsymbol{E}}_1 \mid \hat{\boldsymbol{E}}_2 \mid \hat{\boldsymbol{E}}_3] = \begin{pmatrix} -0.999999 & 0.009155 & -0.010710 \\ -0.000026 & 0.999957 & -0.023833 \\ -0.000004 & -0.001396 & -0.999658 \end{pmatrix}. \tag{51}$$

Clearly the eigen-vector matrix almost coincides with the identify matrix, a fact implying that the POD modes almost coincide with the normal modes of the reduced order system. In view of this result, we pose the question: *Do the POD modes represent Normal Modes of vibration for the full order system?* Since we deal with motions dominated by a single POD mode, we refine this question as follows: *Does at least the dominant POD mode represent (or reflect) a Normal Mode of vibration?*

To answer this question, we explore how the linear natural frequencies of the reduced system change with the energy level varied continuously by changing the magnitude of the impulsive load. Table 5 reveals that RM-frequencies change slightly when the energy level of the free motion is increased. Clearly this has to do with the fact that one mode dominates the motion (Table 6). The shapes of the components of the modes and their norms remain almost constant since the linear natural frequencies remain constant. Table 7 reveals that the ratio of the norms of the transverse and rotatory components remains constant. The above results are compactly reflected into the fact that the eigen-vector matrix

Table 5. The linear natural frequencies of the 3-DOF reduced system.

P	ω_1	ω_2	ω_3
1.00	3078.55	25214.60	60986.46
2.00	3078.57	25214.72	60986.57
4.00	3078.65	25215.16	60987.08
8.00	3078.97	25216.89	60988.95
50.00	3083.97	25249.91	61065.92
100.00	3080.13	25211.42	69023.15

Table 6. The distribution of the auto-correlation energy over the first three POD modes.

P	λ_1	λ_2	λ_3	$\lambda_1+\lambda_2+\lambda_3$
1.00	0.997732	$2.152896E-03$	$1.071543E-04$	0.999992
2.00	0.997734	$2.150906E-03$	$1.062714E-04$	0.999992
4.00	0.997728	$2.156014E-03$	$1.065346E-04$	0.999991
8.00	0.997704	$2.176138E-03$	$1.075710E-04$	0.999987
50.00	0.996841	$2.873136E-03$	$1.447963E-04$	0.999859
100.00	0.995452	$3.974596E-03$	$3.422543E-04$	0.999768

Table 7. The norms of the components of the dominant POD mode.

P	C_{11}	C_{21}	C_{31}
1.00	$9.131084E-005$	0.955687	0.294382
2.00	$1.830379E-004$	0.955688	0.294381
4.00	$3.642348E-004$	0.955688	0.294378
8.00	$7.142191E-004$	0.955692	0.294366
50.00	$2.494674E-003$	0.955812	0.293966
100.00	$2.946818E-003$	0.956019	0.293286

almost coincides with the identity matrix with increasing energy level. Further evidence that the linear natural frequencies of the 3-DOF system are properties of the full order system is presented in Figure 6a revealing the fact that the RM-frequencies for free dynamics excited by a rectangular pulse are close to the ones detected above. Figure 6b reveals that the eigen-matrix coincides with the identity matrix.

The coupling between the axial and the pair transverse-rotatory components is extremely small (Table 7). This sign could reflect the existence of a normal mode of vibration composed of a master part and a slaved part (driven without modal interaction). It is shown in Georgiou [14, 22] that two POD modes are needed to characterize a master-slaved normal mode of vibration. This means that we need at least two POD modes to derive a reduced order model. To assure convergence of the 2-DOF reduced system, we need to augment it by at least one degree-of-freedom by taking into account the next most energetic POD mode. This is one of the reasons we have truncated the reduced system at three-degrees-of-freedom.

To explore whether the free dynamics analyzed above are near an invariant manifold of motion, we compare the impulse response of full order system (1)–(3) to that of 3-DOF reduced system (39).

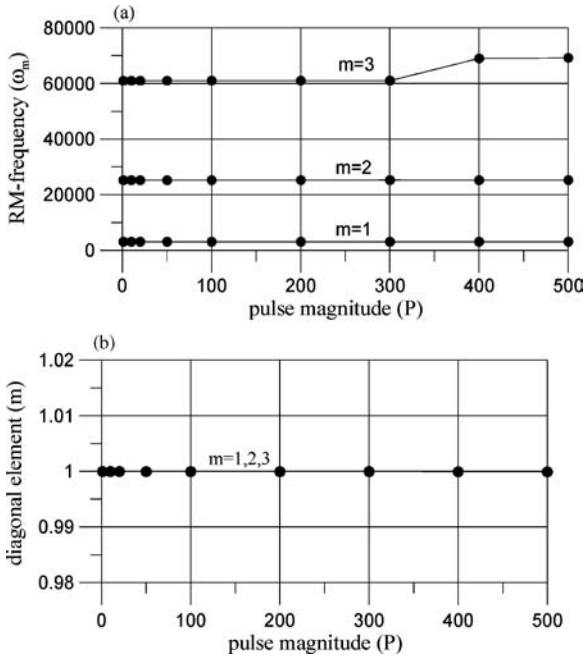

Figure 6. POD-RM analysis of the free dynamics of the planar rod (impulsive load): (a) the linear natural frequencies and (b) the diagonal elements of the eigen-vector matrix of the 3-DOF reduced system.

Clearly near reproduction of the dynamics of the reduced system is a definite sign that the dynamics are close to an invariant subspace of the phase space. Figure 7a reveals that, for low energy levels, the 3-DOF system predicts exceptionally well the dynamics of the full order system. Figure 7b reveals a phase shift in the response of the reduced system at the energy level increases. This is due to the fact that the auto-correlation energy for the transients of free motions is spread over a large number of POD modes. The phase shift shows how much significant are the POD modes with small amount of energy. Nevertheless the dynamics are dominated by the same single POD mode. *The above exercise indicates that the reduced order model provides a valuable tool to determine under what conditions* POD *modes reflect normal modes of coupled systems.*

8. POD-RM Analysis of Motions to Extract the First Normal Mode of Vibration

In this section we derive reduced order models *for attractors* of the full order system dominated by a single POD mode. Since the system is dissipative, these attractors reside in a low-dimensional subspace that may be invariant. The shapes of the POD modes characterize the spatial structure of the subspace uniquely; whereas their amplitudes provide a set of principal coordinates. Clearly the POD structure of an attractor may yield a reduced order model valid over a wide range of systems and forcing parameters. To locate attractors dominated by a single POD mode, we excite the full order system harmonically at single frequencies close to the linear natural bending frequencies of low order (Table 2).

POD-RM analysis of an attractor: We perform a POD analysis of the attractor of the forced motion that starts with zero initial conditions and forcing amplitude at $P = 1$ and frequency at $\Omega = 3121$ rad/s, a value close to the fundamental bending frequency of the linear beam. Notice that this frequency is close

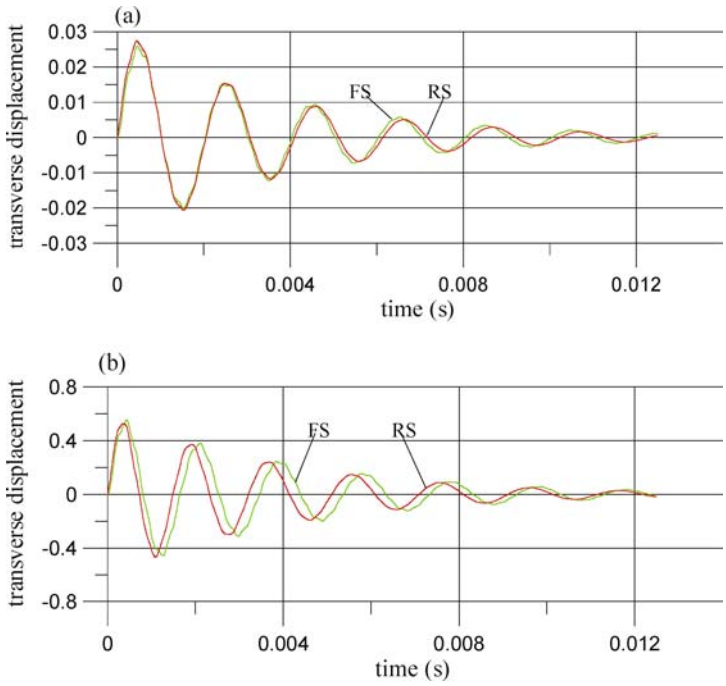

Figure 7. Full order system (FS) *versus* 3-DOF reduced system (RS) for a spatially uniform transverse impulse with magnitude (a) $P = 2$, (b) $P = 50$.

in value to the dominant RM-frequency, Equation (50), of the free dynamics excited by an impulsive transverse load. The attractor is a periodic vibration dominated by a single POD mode. Table 3 presents the norms of the components of the first three most energetic POD modes; whereas Figure 3 depicts the normalized shapes of their components. They are used to derive a 3-DOF reduced system. The numerical values of the mass, dissipation, and stiffness matrices of the 3-DOF reduced system are

$$\begin{aligned}
\boldsymbol{M} &\equiv \begin{pmatrix} M_{11} & M_{12} & M_{13} \\ M_{21} & M_{22} & M_{23} \\ M_{31} & M_{32} & M_{33} \end{pmatrix} = \begin{pmatrix} 9.208166 & -0.000320 & 0.039187 \\ -0.000320 & 10.0000 & -0.004392 \\ 0.039187 & -0.004392 & 6.453854 \end{pmatrix} \times 10^{-7} \\
\boldsymbol{D} &\equiv \begin{pmatrix} D_{11} & D_{12} & D_{13} \\ D_{21} & D_{22} & D_{23} \\ D_{31} & D_{32} & D_{33} \end{pmatrix} = \begin{pmatrix} 5.000000 & -0.000397 & 0.024968 \\ -0.000397 & 5.000000 & -0.000043 \\ 0.024968 & -0.000043 & 5.000000 \end{pmatrix} \times 10^{-4} \\
\boldsymbol{K} &\equiv \begin{pmatrix} K_{11} & K_{12} & K_{13} \\ K_{21} & K_{22} & K_{23} \\ K_{31} & K_{32} & K_{33} \end{pmatrix} = \begin{pmatrix} 0.008730 & 0.00016 & -0.000620 \\ 0.00016 & 4.737673 & -0.005024 \\ -0.000620 & -0.005024 & 0.437346 \end{pmatrix} \times 10^{+3}
\end{aligned} \tag{52}$$

These matrices are full, symmetric and especially positive definite. We have verified these properties for a plethora of free and forced motions of the rod. Therefore, we claim that these properties hold almost for all motions of the rod.

We claim that if an attractor is near an invariant manifold reflecting a normal mode of vibration, its POD structure should contain information on the natural frequencies of the full order system. The

values of the linear natural frequencies (rad/s) of the 3-DOF reduced system are

$$\omega_1 = 3078.89,\ \omega_2 = 68830.80,\ \omega_3 = 26032.04. \tag{53}$$

We notice that the first and third frequencies are respectively close to the first and the third natural bending frequencies of the rod; whereas the second one is very close to the first natural frequency of the linear rod. Recall that the natural frequencies of the linear rod and beam (Table 2) furnish a reasonable approximation to some of the natural frequencies of the full order system. Another interesting result is the fact that the first and the third RM-frequencies (53) are close to the ones for free motions, Equation (50).

For the attractor we have analyzed, the value of the eigen-vector matrix of the 3-DOF reduce system is

$$\hat{\boldsymbol{E}} \equiv \begin{pmatrix} 0.999986 & -0.000034 & 0.001520 \\ -0.000061 & -0.999999 & -0.001124 \\ 0.005108 & 0.001164 & -0.999998 \end{pmatrix}. \tag{54}$$

Matrix (54) almost coincides with the identity matrix. This further implies that the 1-DOF systems corresponding to the three uncoupled POD modes should furnish natural frequencies that are near the RM-frequencies (53). Indeed, these uncoupled natural frequencies are

$$\omega_{10} = 3079.05,\ \omega_{20} = 68830.87,\ \omega_{30} = 26024.25. \tag{55}$$

Therefore, we have $\omega_1 \simeq \omega_{10},\ \omega_2 \simeq \omega_{20},\ \omega_3 \simeq \omega_{30}$. In view of this result, again we pose the question: *Are the POD modes of this motion normal modes of vibration of the full order system?*

We claim that a continuous family of attractors with respect to the forcing parameters should be underlined by a characteristic property if the attractors belong to the same invariant manifold (family of motions). Clearly the linear modes of the 3-DOF reduced system provide such an underlining characteristic property. Table 8 reveals that the eigen-values of the 3-DOF system remain almost constant for forcing frequencies around the first linear natural frequency of the full order system. This is clearly related to the fact that a single POD mode dominates the attractors (Table 9). Table 10 reveals that the norms of the transverse and rotatory components remain constant.

It is a remarkable result the fact that the 3-DOF system of several attractors processes linear natural frequencies close to the ones detected in the free dynamics. This is a sign that the attractor resides on an invariant manifold reflecting a normal mode of vibration of the full order system. Moreover, POD analysis reveals that the axial field is weakly coupled to the other two fields. This property reflects the presence of a master-slave (slow) invariant manifold. We will discuss this issue in detail later.

Table 8. The linear natural frequencies (rad/s) of the 3-DOF reduced system (attractors).

(P, Ω)	ω_1	ω_2	ω_3
10, 2000	3087.00	68852.999	27980.462
1, 3121	3078.99	68830.803	26032.045
10, 3121	3078.88	68830.803	26032.045
10, 4000	3085.83	68843.175	43055.714

Table 9. The distribution of the auto-correlation energy over the first three POD modes (attractors).

(P, Ω)	λ_1	λ_2	λ_3	$\lambda_1 + \lambda_2 + \lambda_3$
10, 2000	0.999481	$4.9183346E-04$	$2.668732E-05$	0.999999
1, 3121	0.999949	$4.9488725E-05$	$8.795890E-07$	0.999999
10, 3121	0.999671	$3.2484900E-04$	$4.491830E-05$	0.999999
10, 4000	0.999613	$3.8160100E-04$	$4.455047E-06$	0.999999

Table 10. The norms of the components of the dominant POD mode (attractors).

(P, Ω)	C_{11}	C_{21}	C_{31}
10, 2000	$1.233980E-003$	0.956316	0.292330
1, 3121	$3.411668E-005$	0.955833	0.293907
10, 3121	$3.696092E-004$	0.956306	0.292367
10, 4000	$3.169742E-005$	0.956451	0.291892

Table 11. The linear frequencies (rad/s) of the 3-DOF reduced system (transient dynamics).

(P, Ω)	ω_1	ω_2	ω_3
1, 2000	3079.35	68831.30	248329.33
10, 2000	3078.46	68832.49	248337.23
1, 4000	3078.92	68836.00	248333.83
10, 4000	3080.20	68862.15	248332.32
20, 3100	3083.43	68829.75	248337.66
80, 3100	3092.99	70525.51	248352.14
200, 3100	3100.96	68912.14	248352.26

POD-RM analysis of transients: If the attractor of a motion resides on an invariant subspace, its dominant POD modes should be present in the transient part of the trajectory of the motion. So we perform a POD analysis of a transient segment of the trajectory of the forced motion whose attractor we have already analyzed. We find that this segment of the motion is dominated by the same POD mode dominating its attractor.

We have performed POD-RM analysis of the transient dynamics of several forced motions. For all analyzed motions, the auto-correlation energy is contained almost exclusively in a single POD mode whose shape is near identically to that dominating the attractor of the motion. Table 11 reveals that the first two RM-frequencies are close to the RM-frequencies of the attractor of the motion (Table 8). The third frequency is close to the ninth frequency of the linear beam. The linear natural frequencies we have detected above are shared by a continuous family of harmonically forced motions over the frequency range [500, 8000] rad/s. This interval contains the dominant RM-frequency of the free dynamics. Figure 8 presents the characteristic properties of the POD-RM analysis of the attractor response; whereas Figure 9 presents the results of the transient response of the forced motions. Notice that the eigen-vector matrix is nearly identical to the identity matrix only over a frequency interval centered at the dominant RM-frequency, which clearly stems from the shape of the dominant POD mode.

The fact that the dominant linear natural frequencies of the reduced system derived from the POD structure of a transient part of a forced motion are close to those of the attractor is a remarkable result,

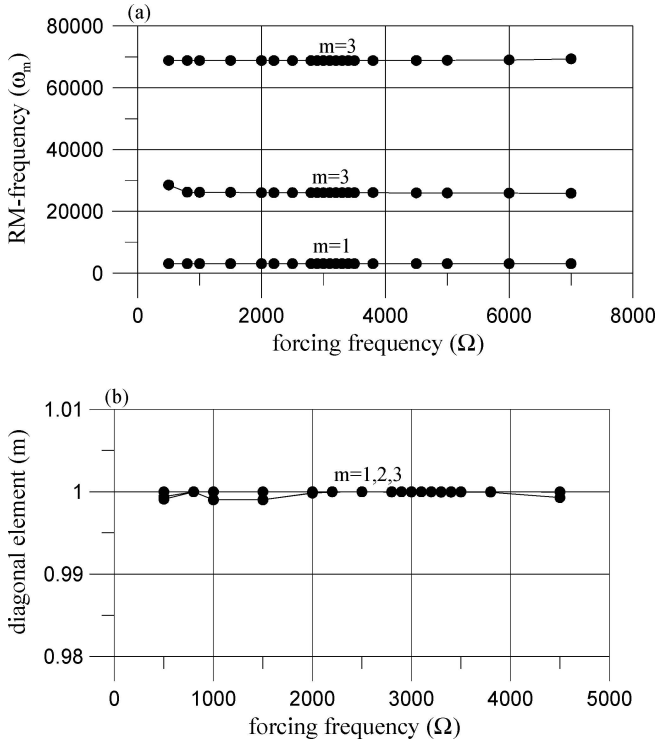

Figure 8. POD-RM analysis of the attractor dynamics of the planar rod over a frequency interval containing the first RM-frequency of the free dynamics (impulsive load): (a) the linear natural frequencies and (b) the diagonal elements of the eigen-vector matrix of the 3-DOF reduced system.

which in turn are near the linear natural frequencies of the full order system. This is a sign that the dominant POD mode of the attractor might represent a normal mode of vibration of the full order system. The dominant POD mode underlines both the free and forced dynamics. Certainly we should consider it to be a characteristic property unifying a large set of motions, a set which could form a two-dimensional invariant manifold for a certain normal mode of vibration.

Another remarkable result is the fact that in a continuous family of attractors with near identical RM-frequencies, some of the attractors possess eigen-vector matrix near the identity one; whereas the rest of them do not processes an eigen-vector matrix near the identity one. *Which one of the attractors is close to a normal mode of vibration? Clearly the one that qualifies the most is the attractor whose eigen-vector matrix is near the identity matrix.*

We conjecture that a motion close to a normal mode of vibration contains the POD structure of the invariant manifold related to that normal mode. A sign that a given motion is close to a normal mode is near containment of the auto-correlation energy at a single POD mode. We do not claim that any motion characterized by a single POD is necessarily close to a normal mode of vibration. The eigen-vector structure of the reduced system furnishes an additional criterion to decide whether a single-POD mode motion is near a normal mode of vibration.

8.1. The 3-DOF Reduced System versus the Full Order System

In this section we integrate numerically the 1, 2, 3-DOF reduced order systems and compare their response to the full order system. Near reproduction of the dynamics of the full order system by the

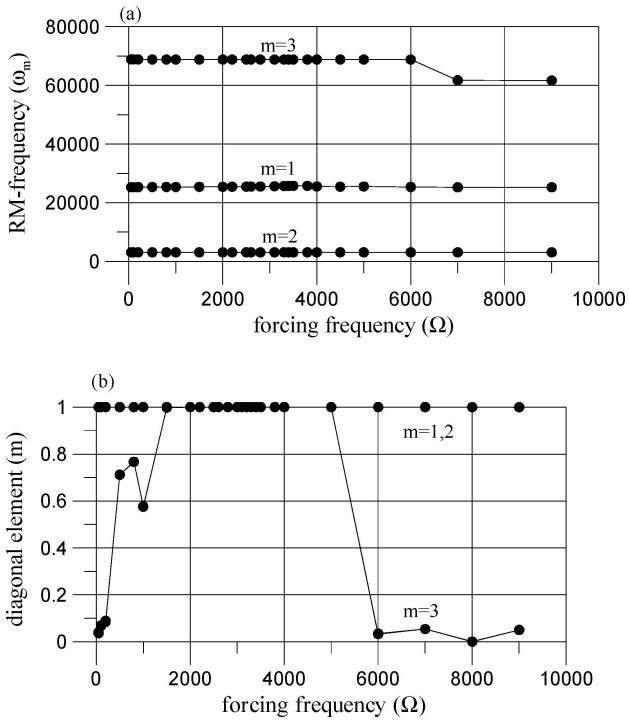

Figure 9. POD-RM analysis of the transient dynamics of the planar rod over a frequency interval containing the RM-frequency for the free dynamics (impulsive load): (a) the linear natural frequencies and (b) the diagonal elements of the eigen-vector matrix of the 3-DOF reduced system.

reduced system is a definite sign that the attractor is near an invariant manifold. The 1, 2, 3-DOF reduced systems are based on the POD structure of the attractor of the forced motion at amplitude $P = 1.0$ and frequency at $\Omega = 3100.0$ rad/s. Both the reduced order and full order systems are compared for harmonic forcing at zero initial conditions. Figure 10 reveals that the agreement between the reduced and full order systems is excellent. The simulations include the transient and attractor parts of the motion. This is a definite sign that the dynamics of the full order system wander near a two-dimensional invariant manifold reflecting the first normal mode of vibration.

We have derived a reduced order system for motions presumably near the first (fundamental) normal mode of vibration of the full order system. The POD analysis reveals that these motions interact weakly only with higher normal modes of vibration. This is reflected directly in the near-identity structure of the eigen-vector matrix of the attractors of harmonically forced motions over a wide range of forcing parameters. Motions near higher normal modes of vibration interact with both lower and higher order modes. If they are very close to a normal mode of vibration they should be dominated by a single POD mode. We proceed to explore the properties of forced motions at frequencies close to the third and fifth normal modes of the full order system. We use the POD-RM analysis as an identification tool to explore whether the attractors of these motions are close to a normal mode of vibration.

9. POD-RM Analysis of Motions to Extract the Third and Seventh Normal Modes of Vibration

Before we apply the POD-RM procedure to analyze a certain set of forced motions to extract the shape of the third normal of vibration, we analyze in detail the attractor and transient segments of the trajectory

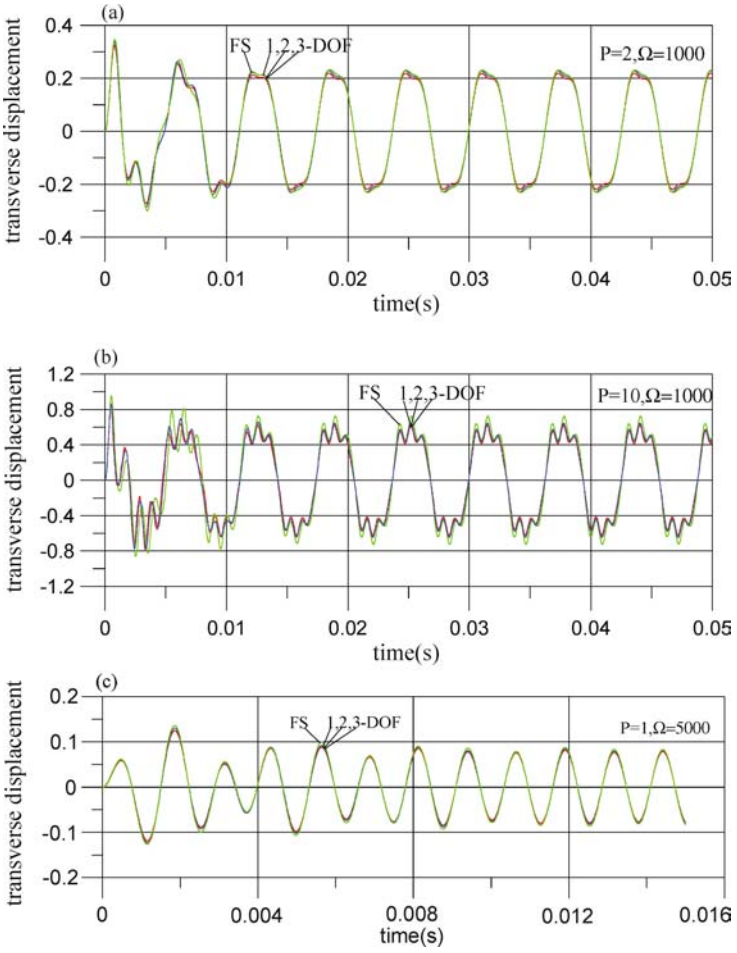

Figure 10. Full order system versus reduced order systems for harmonic forcing at frequencies below (a) and (b) and above (c) the dominant linear natural frequency of the 3-DOF reduced system.

of a specified forced motion of the rod. The forcing is harmonic at amplitude $P = 1$ and frequency $\Omega = 28000$ rad/s, a value close to the third natural frequency of the linear beam. With this harmonic forcing, we expect to excite vibrations close to the third normal mode.

POD-RM analysis of an attractor: The attractor of this forced motion is a periodic vibration and is dominated by a single POD mode. Table 4 presents the POD analysis of this attractor; whereas Figure 4 gives the normalized shapes of the three first POD modes. We use these modes to derive a 3-DOF reduced system. It turns out that the mass, dissipation, and stiffness matrices of this reduced system are symmetric and positive definite. The linear natural frequencies (rad/s) of the reduced system are

$$\omega_1 = 2521.90,\ \omega_2 = 5046.33,\ \omega_3 = 97939.93. \tag{56}$$

We notice that the dominant frequency is nearly identical to the second natural frequency of the reduced system for the free dynamics. The second one lies between the first and second frequency of the linear beam. The third frequency is close to the third frequency of the linear rod. The linear natural frequencies of the reduced system must be related to the linear natural frequencies of the full order system. We

assume that for each level of potential energy the full order system has distinct normal modes and thus distinct natural frequencies (up to a certain critical level).

We examine the eigen-vector matrix of the 3-DOF reduced system to extract additional information. The value of this matrix is

$$\hat{\boldsymbol{E}} = \begin{pmatrix} 0.923442 & 0.385599 & 0.000119 \\ 0.383737 & -0.922666 & -0.000079 \\ -0.000032 & 0.000070 & -0.999999 \end{pmatrix}. \tag{57}$$

Clearly matrix (56) is not close to the identity matrix. In particular, the first two eigenvectors do not coincide with the principal directions. This is due to the substantial inertial and stiffness coupling between any two POD modes. *It seems that a rotation about the third principal direction*, *which corresponds to the least energetic POD mode, can map the eigen-vector matrix into the identity one*.

Here we have a motion characterized by a single POD mode but its eigen-vectors do not coincide with the principal directions provided by the POD modes. We pose the question: *Does this motion contain information regarding the nearby presence of a normal mode of vibration (two-dimensional invariant manifold)?* We proceed to explore whether the RM-frequencies (55) underline a family (category) of attractors. Tables 12–14 present the results of a POD-RM analysis for several attractors for motions forced at $\Omega = 28000$ rad/s and various amplitudes. Table 12 shows that the RM-frequencies change slightly over an interval of forcing amplitude. This is clearly due to the fact that the motion is dominated by a single mode (Table 13). Moreover, the axial component of the dominant POD mode is weakly coupled to the transverse and rotatory components whose ratio is almost constant (Table 14). The weak coupling between the axial and the other components may reflect the existence of a master-slaved type of normal mode.

We have explored how the RM-frequencies (56) vary for attractors of harmonically forced motions at frequencies over the interval [10000, 40000] rad/s. Notice that the interval contains the dominant RM-frequency $\omega_1 \simeq 25222.00$ rad/s. Figure 11a reveals that the first two RM-frequencies remain almost constant over a frequency sub-internal that contains a characteristic frequency for which, as Figure 11b reveals, the eigen-vector matrix is near the identity one. This characteristic frequency is the dominant RM-frequency and is shared by all attractors. Notice that away from this characteristic frequency the eigen-vector matrix deviates substantially away from being near the identity matrix. This deviation turns out to be a well-defined rotation about the principal direction of the least energetic POD mode.

Table 12. The linear natural frequencies of the 3-DOF reduced system (attractors).

P	ω_1	ω_2	ω_3
0.20	2521.936	5096.526	96101.255
0.50	2521.937	5096.486	96102.183
1.00	2521.936	5096.365	96105.494
5.00	2521.934	5092.407	96208.185
10.00	2521.927	5079.802	96540.432
20.00	2521.903	5025.180	98067.694
40.00	2523.248	3881.160	159655.464
70.00	2523.828	3732.526	130638.830
100.00	2524.564	3591.576	114760.227

Table 13. The distribution of the auto-correlation energy over the first three POD modes (attractors).

P	λ_1	λ_2	λ_3	$\lambda_1+\lambda_2+\lambda_3$
0.20	0.998948	$1.05165E-003$	$5.427609E-009$	0.999999
0.50	0.998948	$1.05167E-003$	$3.392289E-008$	0.999999
1.00	0.998948	$1.05176E-003$	$1.356968E-007$	0.999999
5.00	0.998942	$1.05438E-003$	$3.396257E-006$	0.999999
10.00	0.998923	$1.06275E-003$	$1.363453E-005$	0.999999
20.00	0.998844	$1.09992E-003$	$5.543196E-005$	0.999999
40.00	0.997267	$2.31668E-003$	$3.946757E-004$	0.999978
70.00	0.996806	$2.38313E-003$	$7.676596E-004$	0.999956
100.00	0.996283	$2.38791E-003$	$1.247831E-003$	0.999919

Table 14. The norms of the components of the dominant POD mode (attractors).

P	C_{11}	C_{21}	C_{31}
0.20	$3.198184E-007$	0.8084543	0.588559
0.50	$7.996684E-007$	0.8084534	0.588560
1.00	$1.599375E-006$	0.8084499	0.588564
5.00	$8.002491E-006$	0.8083301	0.588729
10.00	$1.604017E-005$	0.8079476	0.589254
20.00	$3.240958E-005$	0.8062883	0.591522
40.00	$6.009119E-005$	0.7869084	0.617069
70.00	$1.004029E-004$	0.7943530	0.607456
100.00	$1.334917E-004$	0.8031443	0.595784

In view of the above results, it seems that the dominant RM-frequency is an approximation to the natural frequency of a normal mode of vibration of the full order system. This frequency should stem exclusively from the shape of the dominant POD mode of certain attractor. Figure 12, however, reveals that the shape of the dominant POD mode does not remain constant as a function of forcing frequency. This was not the case with the first normal mode of vibration whose underlining POD mode processes components with constant norms. Nevertheless, this dominant RM-frequency should be present in the transient response of a forced motion.

POD-RM analysis of transients: It turns out that the transient dynamics of the motion (forcing amplitude $P = 1$ and frequency $\Omega = 28000$ rad/s) whose attractor was analyzed above is domintated by a single POD mode. The linear natural frequencies of the corresponding 3-DOF reduced system have the following values (rad/s):

$$\omega_1 = 25215.64,\ \omega_2 = 3106.23,\ \omega_3 = 61514.12. \tag{58}$$

We notice that the dominant RM-frequency (58) is very close to the dominant RM-frequency of the attractor (56). We cannot help noticing that the second RM-frequency, $\omega_2 = 3106.23$, is close to the first linear natural frequency of the full order system. We shall see that the third RM-frequency, $\omega_3 = 61514.12$, is an approximation to a natural frequency of the full order system.

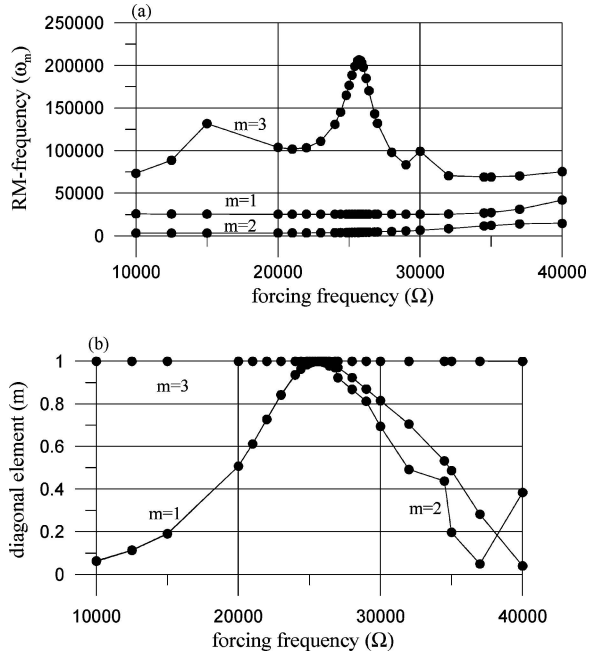

Figure 11. POD-RM analysis of the attractor dynamics of the planar rod over a frequency interval containing the second RM-frequency for the free dynamics (impulsive load): (a) the linear natural frequencies and (b) the diagonal elements of the eigen-vector matrix of the 3-DOF reduced system.

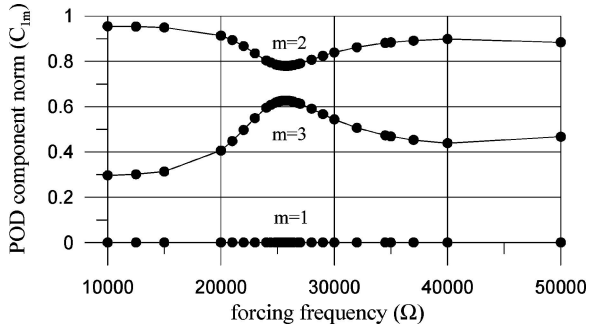

Figure 12. The distribution of the norms of the components of the dominant POD mode.

The value of eigen-vector matrix of the 3-DOF reduce system is

$$\hat{\boldsymbol{E}} \equiv \begin{pmatrix} 0.943291 & 0.332567 & 0.019222 \\ -0.331756 & 0.942529 & 0.027385 \\ -0.011792 & -0.032207 & 0.999440 \end{pmatrix}. \tag{59}$$

It is not close by any means to the identity matrix. Just as for the care of the attractor of the motion, it is clear that a rotation about the third eigen-vector maps matrix (59) near the identity one.

We have performed a POD-RM analysis of the transient dynamics of the attractors listed in Tables 12–14 to find that a single POD mode dominates the dynamics. Table 15 reveals that the RM-frequencies remain constant over a range of forcing amplitude. Notice that above some critical

Table 15. The linear natural frequencies of the 3-DOF reduced system for the transient dynamics for harmonic forcing at frequency close to the third linear bending one.

P	ω_1	ω_2	ω_3
0.50	2521.649	3106.642	61512.636
1.00	2521.649	3106.704	61512.881
5.00	2521.653	3108.636	61519.924
10.00	2521.662	3113.140	61535.870
20.00	2521.709	3120.698	61570.414
40.00	2523.358	3730.073	163547.833
70.00	2524.290	3771.580	123616.473
100.00	2525.014	3682.507	102142.704

Table 16. The norms of the components of the dominant POD mode for the transient dynamics for harmonic forcing at frequency close to the third linear bending one.

P	C_{11}	C_{21}	C_{31}
0.50	$8.206170E-006$	0.8018712	0.597496
1.00	$1.638127E-005$	0.8018661	0.597503
5.00	$7.708031E-005$	0.8016943	0.597734
10.00	$1.269841E-004$	0.8011320	0.598487
20.00	$1.055944E-004$	0.7986324	0.601819
40.00	$5.674124E-005$	0.7847297	0.619838
70.00	$1.190102E-004$	0.7911465	0.611626
100.00	$9.202301E-005$	0.7990360	0.601283

amplitude the third frequency changes. This is clearly due to the fact that the system is nonlinear and thus the natural frequency associated with a normal mode of vibration varies with the energy level. Figure 13 shows the normalized shapes of the components of the dominant mode, whose norms remain constant over a range of forcing amplitude (Table 16).

To determine how the RM-frequencies depend on the forcing frequency, we have performed a POD-RM analysis for the transients of harmonically forced motions at frequencies over the range [10000,

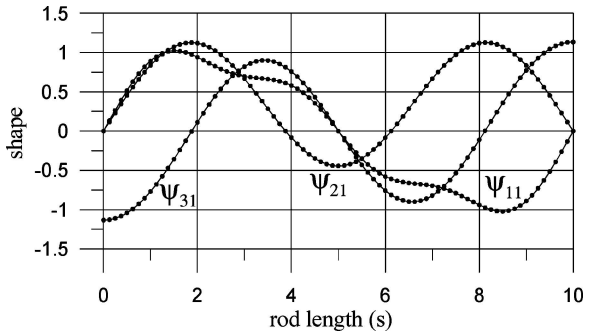

Figure 13. The normalized components of the dominant POD mode underlining the transient response.

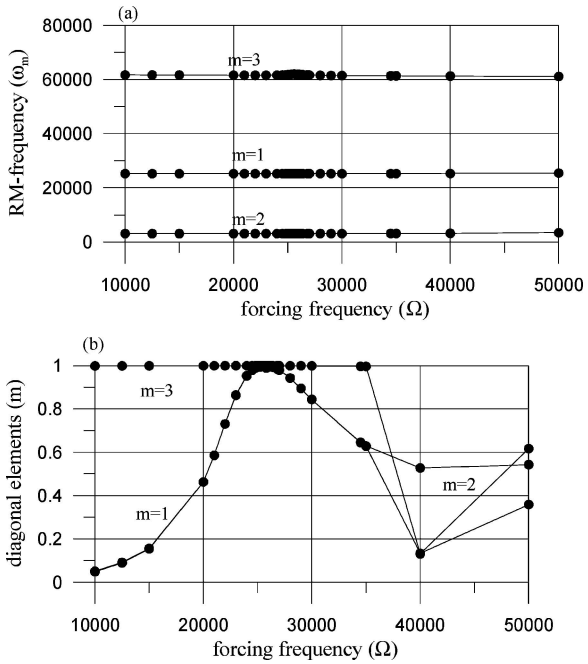

Figure 14. POD-RM analysis of the transient dynamics of the planar rod over a frequency interval containing the RM-frequency of the 3-DOF reduced system for the free dynamics (impulsive load): (a) the linear natural frequencies and (b) the diagonal elements of the eigen-vector matrix of the 3-DOF reduced system.

40000] rad/s and forcing amplitude fixed at $P = 1$. This interval contains the dominant RM-natural frequency. Figure 14a reveals that the RM-frequencies remain nearly constant over the entire frequency range; whereas the eigen-vector matrix, as Figure 14b reveals, approaches the identity matrix over a short interval centered at the dominant RM-frequency.

The remarkable result is the fact that all the RM-frequencies are close to certain natural frequencies of the linear rod and beam, which are approximations to the linear natural frequencies of the full order system (planar rod). The other remarkable result is the fact that these motions are dominated by a single POD mode whose component norms do not remain constant (Figure 12). We conjecture that the variation of the component norms manifest itself as a rotation of the eigen-vector matrix. *Could the dominant RM-frequency and therefore the POD mode from which it stems be related to a normal mode of vibration of the full order system?* To answer this question, we compute an attractor diagram for motions with zero initial conditions for a frequency sweep at constant amplitude level over an interval centered at the dominant RM-frequency. We obtain information on the attractor of a motion by computing the long term iterates of the Poincare section of the transverse displacement at the middle of the rod. The Poincaré map is computed by integrating the finite element model of the rod. Figure 15, which is an attractor diagram, reveals the existence of a resonant frequency close to the dominant RM-frequency.

With this information at hand, we perform a reduced model POD analysis of the attractors of motions excited at frequencies close to the dominant RM-frequency. The result is *the common dominant RM-frequency is an approximation to a resonant frequency of the full order system.* Another remarkable result is the fact that the eigen-vectors almost coincide with the principal directions. For example, for the attractor of a forced motion at amplitude $P = 1.0$ and frequency $\Omega = 25700.00$ rad/s the eigen-vector

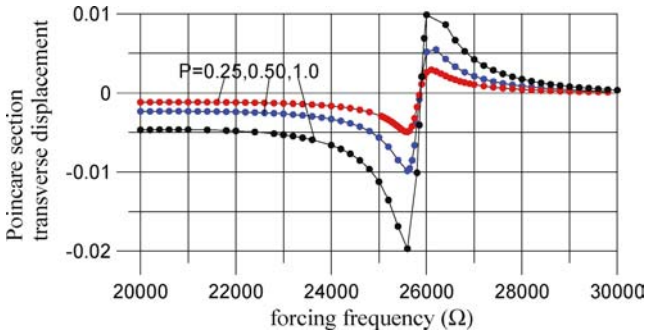

Figure 15. Frequency attractor diagrams for the full order system at three amplitude levels reveals the existence of a resonant frequency close to the dominant linear frequency of the 3-DOF reduced system.

matrix is

$$\hat{\boldsymbol{E}} \equiv \begin{pmatrix} 0.999998 & 0.002919 & 0.000270 \\ -0.001418 & 0.999995 & 0.0000039 \\ -0.000009 & 0.0000008 & -0.999999 \end{pmatrix}. \tag{60}$$

Matrix (59) reveals that the eigen-vectors almost coincide with the principal directions. This is a very interesting result since forced motions at a frequency away from a resonant frequency are dominated by a single POD mode but the eigen-vectors of the reduced system do not coincide with the principal directions.

Up to this point we have clear evidence how the POD-RM analysis determines when a motion dominated by a single POD mode is related to a normal mode of vibration. The POD-RM method can be applied to extract from a certain category of motions the frequencies and the shapes of normal modes of vibration. For example, we have applied the POD-RM analysis to identify the seventh normal mode (numbered according to the modes of the linear rod and beam) of the full order system. Figure 16 presents the results of the POD-RM analysis for a frequency sweep at amplitude level $P = 0.50$ over the frequency range [50000, 70000] rad/s. The dominant RM-frequency is $\omega \simeq 6121.00$ rad/s. This is near the third of the RM-frequencies (50) of the free dynamics excited by a spatially uniform transverse load of pulse type. It turns out that this frequency approximates a resonant frequency of the full order system.

The conclusion is *that the shape of the normal mode of vibration is given by the single dominant POD mode of that attractor whose eigen-vector matrix coincides with the identity matrix.* The fact that at resonance the eigen-vectors of the reduced system coincide with the principal directions explains completely why in all free motions we found a reduced model whose eigen-vectors almost coincide with the principal directions. This suggests that a systematic way to search for relations between the POD modes and normal modes of vibration is to perform a POD-RM analysis of the free dynamics. Figure 17 presents the shapes of the first, third and seventh normal modes of vibration; whereas Table 17 presents the norms of their components. Notice that the transverse component of these normal modes is precisely a 90 degrees shift of the transverse component.

10. Predictability of the 3-DOF Reduced System

If the 3-DOF reduced system represents the dynamics on an invariant manifold, it should be able to reproduce faithfully the dynamics of the full order system over a relatively wide range of forcing

Table 17. The norms of the components of the normal modes extracted by a POD-RM processing of a certain category of motions.

Mode order	Axial (C_{11})	Transverse (C_{21})	Rotatory (C_{31})
1st	$1.06740E-005$	0.955827	0.293928
3rd	$8.97817E-006$	0.779691	0.626164
7th	$6.28669E-007$	0.678027	0.735036

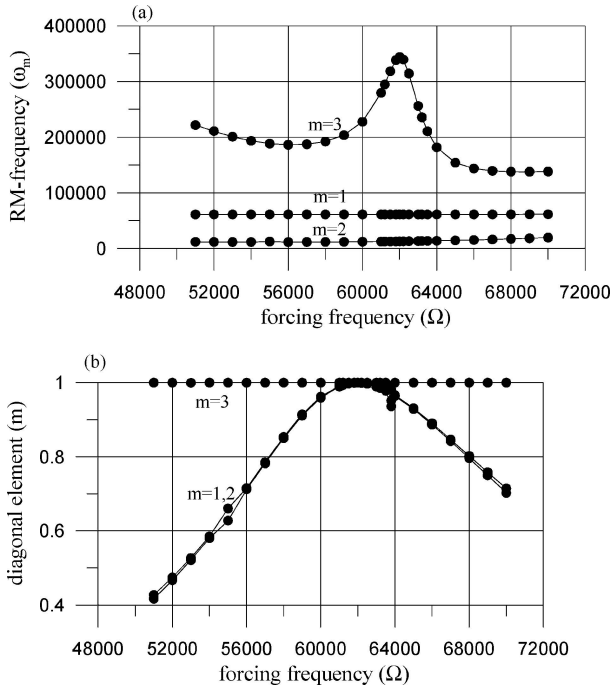

Figure 16. POD-RM analysis of the attractor dynamics of the planar rod containing the third RM-frequency of the free dynamics (impulsive load): (a) the linear natural frequencies and (b) the diagonal elements of the eigen-vector matrix of the 3-DOF reduced system.

parameters. The forcing frequency should be varied in an interval centered at the resonant frequency stemming from the normal mode of vibration.

Here we present some results on the predictability of the 3-DOF reduced order system at different values of the properties for which it was derived. We compute Poincaré sections of the attractor of a motion with zero initial conditions as a function of a forcing parameter while keeping constant the other one. Figure 18a is an amplitude sweep attractor diagram at constant forcing frequency; whereas Figure 18b is a frequency sweep at constant amplitude level. Clearly the reduced order system predicts exceptionally well the dynamics of the full order system over a wide range of forcing parameters.

For low-frequency harmonic excitation, the reduced system reproduces the dynamics of the full order system over a wide range of forcing parameters. For example, Figure 18c reveals how accurately the reduced system captures the qualitative dynamics of the full order system at very low frequencies. It is worth mentioning that the 1-DOF reduced system predicts reasonably well the almost static response of the full order system. We computed the almost static response by forcing the systems at very low

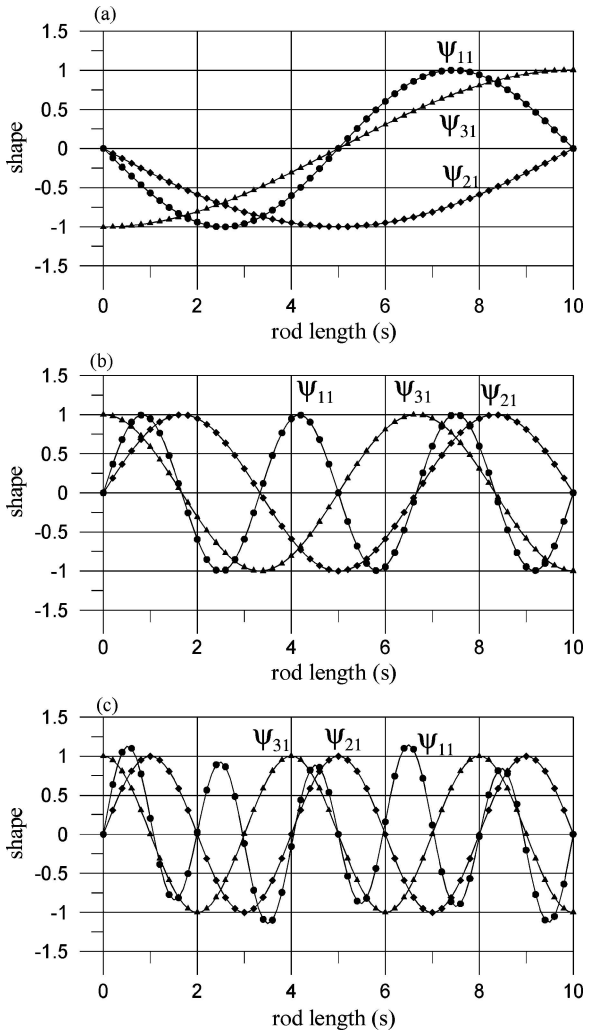

Figure 17. The normalized shapes of the components of (a) the 1st, (b) the 3rd and (c) the 7th normal modes of vibration realized as the single dominant POD of a forced vibration.

frequency with respect to the first natural frequency. Recall that the first natural frequency of the rod is at $\omega \simeq 3080.00$ rad/s. Figure 19 compares the responses of the full order and the reduced order systems at very low-frequency harmonic excitation ($\Omega = 50$ rad/s).

11. Signs of Slow Invariant Manifolds

Linearized equations of motion (22) prompt us to consider our full order system (1)–(3) as one composed of a high frequency-subsystem and a low frequency-subsystem. The high frequency, also called stiff, subsystem is the equation governing the longitudinal displacement field; whereas the low frequency, also called soft, subsystem is the coupled equations governing the transverse displacement and the in-plane rotation of the cross-section of the rod. Because of the wide gap between the fundamental

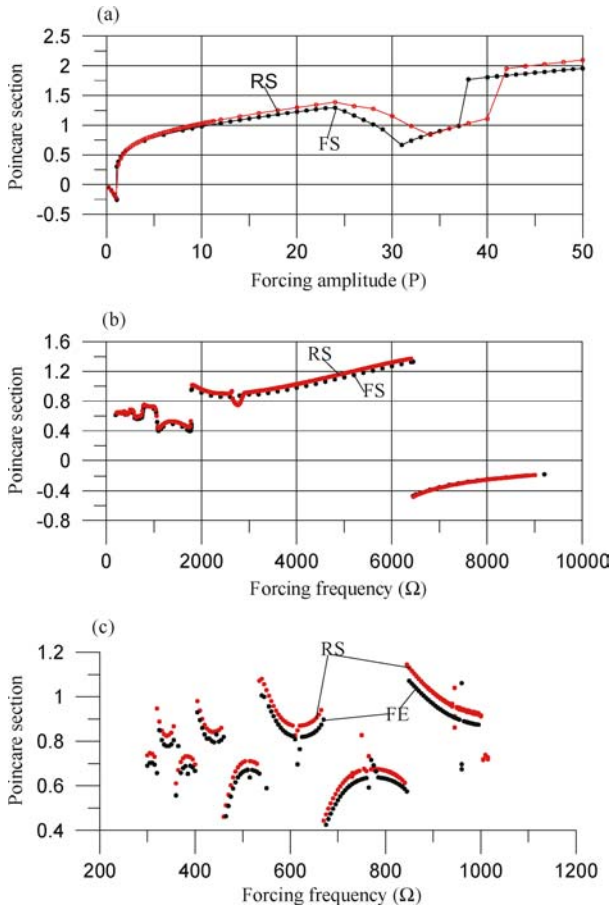

Figure 18. Prediction by the 3-DOF reduced system (RS) and the finite element model of the full order system (FE, FS): (a) amplitude sweep attractor diagram at forcing frequency 4000 rad/s, (b) frequency sweep attractor diagram at amplitude level $P = 10$, (c) frequency sweep attractor diagram at amplitude level $P = 15$.

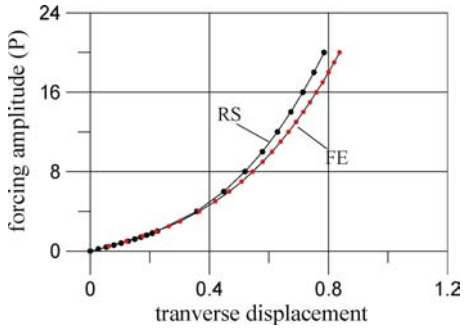

Figure 19. Amplitude sweep attractor diagram at very low frequency predicted by the 1-DOF reduced system (RS) and the finite element model of the full order system (FE).

linear frequencies for longitudinal vibrations and bending-shearing vibrations, the stiff subsystem is weakly coupled to the soft subsystem and vice versa. Indeed, the POD analysis reveals that a steady state motion (coupled vibration) is composed of a number of POD modes whose both the transverse and rotational components dominate over the axial component and a number of POD modes

whose axial component dominates over both the transverse and rotational components. For instance, Table 2 shows that the dominant POD mode is essentially a bending-shearing motion; whereas the second mode is essentially a longitudinal motion.

We therefore have a stiff/soft infinite system with multi-field dynamics. The dynamics of such systems evolve on slow and fast time scales. The phase space of such systems contains global invariant manifold with dimension less or equal to that of the soft subsystem. It has been found that coupled stiff/soft infinite systems in mechanics possess low-dimensional slow invariant manifolds [17]. A two-dimensional slow invariant manifold stems from a normal mode of the uncoupled slow subsystem. The prototypical stiff/soft coupled system used to validate this fact was a planar pendulum coupled to a cantilevered beam. For this system the slow invariant manifold is two-dimensional and it represents a global slow normal mode of vibration composed of a master part and slaved part. The basic frequency of the slaved part is twice that of the master part [17, 26]. As a result of this frequency relation such a normal mode of vibration is *not synchronous*, and therefore appears as an inseparable pair of two POD modes. The master POD mode dominates over the shaved one. This has been shown theoretically and verified experimentally using a beam/pendulum system [25].

A way to explore whether the categories of motions we have studied contain master and slaved vibrations, thus a definite sign of an underlining slow invariant manifold, is to look for a functional relationship between the amplitude of the dominant POD mode and the amplitude of any other POD mode. The categories of motions we have studied are indeed characterized by master and slaved POD modes. We have already seen that this relationship is reflected in the weak coupling of the axial field to the transverse and rotational fields. For forcing at low frequencies around the first natural frequency, the steady state motions (vibrations) are dominated by a single POD mode. The master mode is the dominant POD mode. Figure 20 reveals that the amplitude of the second POD mode is a function of the amplitude of the dominant POD mode. This is a definite sign of a master-slaved relation between the dominant and the second POD mode. This relation is reflected into the fact that the frequency of the amplitude of the second POD is precise twice that of the amplitude of the master POD mode. Figure 21 reveals that such a master-slave relationship is also found between the amplitude of the third, now, POD mode and that of the dominant POD mode for the second category of forced vibrations, which are close to the third normal mode of vibration. Needless to say that the master-slaved relationship is present in the forced vibrations at frequencies close to the natural frequency of the seventh normal mode of vibration. It seems that the master-slaved relation is an underlining property of forced vibrations at frequencies near the natural frequencies. For the three categories of motions we have analyzed, the slaved amplitude has frequency twice that of the master amplitude.

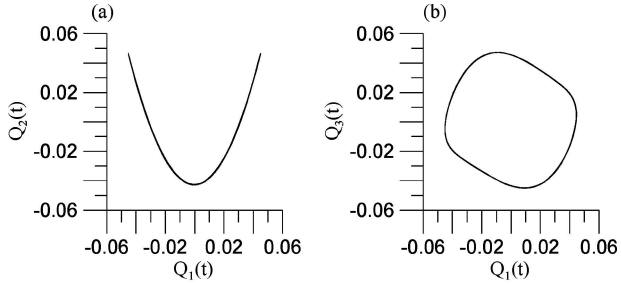

Figure 20. Cross plotting of (a) the amplitude of the second POD mode and (b) the amplitude of the third POD mode against the amplitude of the dominant POD mode for the attractor of a forced motion at a frequency near that of the first normal mode of vibration.

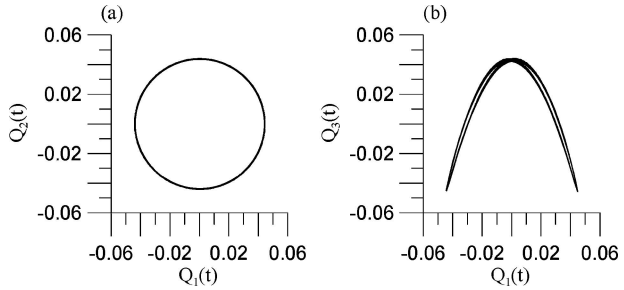

Figure 21. Cross plotting of (a) the amplitude of the second POD mode and (b) the amplitude of the third POD mode against the amplitude of the dominant POD mode for the attractor of a forced motion at a frequency near that of the third normal mode of vibration.

If there exists a slow invariant space in the phase space of the 3-DOF reduced system, the amplitude of the slaved part must be a single-valued function of the amplitude and velocity of the master part of the manifold and, for nonzero forcing, depending parametrically on the forcing. That for a motion on the slow manifold the second POD mode is slaved to the first POD mode means precisely the following:

$$\begin{aligned} Q_2(t) &= f_\mu(Q_1(t), \dot{Q}_1(t), t; P, \Omega), \\ \dot{Q}_2(t) &= g_\mu(Q_1(t), \dot{Q}_1(t), t; P, \Omega). \end{aligned} \tag{61}$$

The parameter μ is a dimensionless frequency that designates the level of coupling between the master and slaved modes.

The slow invariant manifold should be exponentially attractive meaning that the attractor of a motion will land on the manifold in the long term provided that the forcing frequency is relatively close to the resonant frequencies of the slow subsystem.

To determine whether the attractors of forced motions dominated by single POD modes satisfy the above relation, that is they reside on a slow invariant manifold, we compute attractor diagrams for the 3-DOF reduced system by means of Poincaré sections. The Poincaré section at the period of the forcing eliminates the time dependence in Equation (61). Figure 22a reveals a single-valued function relation between the assumed slaved and master parts for a frequency sweep attractor diagram over the interval [2000, 5000] rad/s. Notice that this interval contains the linear natural frequency of the first normal mode of vibration. Figure 22b reveals a single-valued function relation between the assumed slaved and master parts of the 3-DOF system for an amplitude sweep over the interval [1, 50] at a fixed frequency relatively near the linear natural frequency of the first normal mode of vibration.

We clearly see the master-slaved relation among the dominant POD and another POD mode in the first three POD modes used to derive the 3-DOF reduced system. The slow invariant manifold is an important characteristic property of the system. When it becomes unstable, interaction among the soft and stiff subsystems is activated. The system also possesses at least one fast invariant manifolds of motion. The normal mode structure of the 3-DOF systems can be studied further by applying the theory of geometric singular perturbations [29, 30]. In a series of works, this author and co-workers [17, 25, 30] have shown that the formulation of coupled structural/mechanical problems as singular perturbation problems furnishes a very basic geometric framework to seek effectively the roots of normal modes of coupled systems in the normal modes of uncoupled soft and stiff sub-systems.

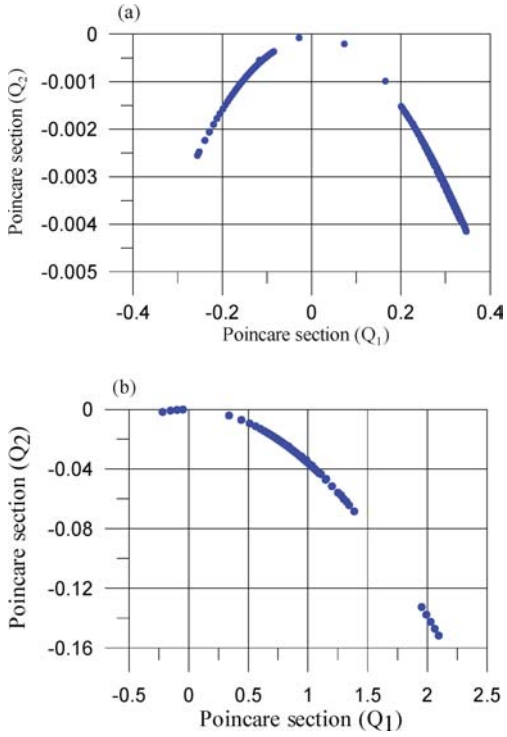

Figure 22. Attractor diagrams predicted by the 3-DOF reduced system for the first normal mode of vibration: (a) frequency sweep attractor, (b) amplitude sweep attractor. The amplitude of the second POD mode is a single-valued function of the state of the first (dominant) POD mode. This relationship is evidence of an attractive global slow invariant manifold.

12. Conclusions and Discussion

This work presented a methodology to characterize the dimensional complexity of the dynamics of a geometrically exact nonlinear rod restricted to move in a plane. The basic tool for the complexity analysis is the method of proper orthogonal decomposition for coupled fields. The POD analysis characterizes a motion in terms of proper orthogonal modes and the auto-correlation energy spectrum. To further refine the characterization of coupling complexity in terms of normal modes of vibration, we derive reduced order models by Galerkin projection of the coupled equation of motion onto the POD modes. The structure of the mass, dissipation, and stiffness matrices reveals how the POD modes are coupled to each other in a multi-field dynamical system. We use the reduced models as an advanced POD tool to search for unknown relations between POD modes and normal modes of vibration for the categories of motions whose POD spectrum is concentrated on a single POD mode. Free dynamics with appropriate initial conditions and forced motions near resonances give rise to motions dominated by a single POD mode. For these motions we derive a three-degree-of-freedom reduced system to capture the coupling of the dominant POD mode to the POD modes with extremely small energy content. This coupling is captured elegantly by the elements of the mass, dissipation, and stiffness matrices of the reduced system. The remarkable result is the fact that for certain free and forced motions the eigen-vectors of the linearized reduced system almost coincide with the principal directions provided by the amplitudes of the POD modes. This is taken as a definite sign that the dominant POD mode is near a normal mode of vibration. The nearness can be quantified since the energy content of the POD

modes is known. We have seen this to be also true for resonant steady state motions (attractors) close to the first, third, and seventh resonant bending frequencies of the rod. It is worth mentioning that the mass and stiffness matrices of the reduced system determine the resonant frequencies of the full order system.

A single POD mode characterizes all forced motions for forcing frequencies over an interval containing the resonant frequency. The POD structure of any of these motions gives almost identical reduced models. This is a clear reflection of the fact that the dominant POD mode is close to a normal mode of vibration. The reduced model reproduces faithfully the dynamics of the full order system for a wide range of parameters of a harmonic forcing. This strongly indicates the fact that these motions reside near an invariant manifold representing a normal mode of vibration. Indeed, numerical analysis reveals that the reduced order model possesses a slow invariant manifold. Due to the fact that the auto-correlation energy is almost contained in a single mode, we claim that the slow invariant manifold is a very small perturbation of a dominant two-dimensional invariant manifold. The dominant slow invariant manifold forms the signature for a normal mode of vibration.

The POD-based reduced model method presented here is a basic result of a Proper orthogonal decomposition approach aiming at identifying the shapes of normal modes of vibration of coupled structural systems with arbitrary physical domains and boundaries. We have chosen geometrically exact rods to determine existing relations between POD modes and normal modes of vibration.

Appendix

The nonlinear term in Equation (25) is given by

$$\boldsymbol{L}_{EL}[\boldsymbol{V}(s,t)] = [L_{\mathrm{ELA}}, L_{\mathrm{ELT}}, L_{\mathrm{ELR}}]^{\mathrm{T}}, \tag{A.1}$$

where L_{ELA}, L_{ELT}, L_{ELR} designate axial, transverse, and rotatory components. The axial component is given by

$$L_{\mathrm{ELA}} \equiv f_1 \sin(\theta_3(s,t)) + f_2 \sin^2(\theta_3(s,t)) + f_3 \cos^2(\theta_3(s,t)) + f_4 \sin(\theta_3(s,t)) \cos(\theta_3(s,t)), \tag{A.2}$$

where

$$\begin{aligned}
f_1 &\equiv -EA\frac{\partial \theta_3(s,t)}{\partial s},\\
f_2 &\equiv -GA\frac{\partial^2 u_1(s,t)}{\partial s^2} + [EA - GA]\frac{\partial u_2(s,t)}{\partial s}\frac{\partial \theta_3(s,t)}{\partial s},\\
f_3 &\equiv -EA\frac{\partial^2 u_1(s,t)}{\partial s^2} - [EA - GA]\frac{\partial u_2(s,t)}{\partial s}\frac{\partial \theta_3(s,t)}{\partial s},\\
f_4 &\equiv -[EA - GA]\frac{\partial^2 u_2(s,t)}{\partial s^2} + 2[EA - GA]\left[1 + \frac{\partial u_1(s,t)}{\partial s}\right]\frac{\partial \theta_3(s,t)}{\partial s}.
\end{aligned} \tag{A.3}$$

The transverse component is given by

$$L_{\mathrm{ELT}} \equiv g_1 \cos^2(\theta_3(s,t)) + g_2 \sin(\theta_3(s,t)) \cos(\theta_3(s,t)) + g_3 \sin^2(\theta_3(s,t)), \tag{A.4}$$

where

$$g_1 \equiv -GA\frac{\partial^2 u_2(s,t)}{\partial s^2} - [EA - GA]\left[1 + \frac{\partial u_1(s,t)}{\partial s}\right]\frac{\partial \theta_3(s,t)}{\partial s},$$
$$g_2 \equiv -[EA - GA]\frac{\partial^2 u_1(s,t)}{\partial s^2} - 2[EA - GA]\frac{\partial u_2(s,t)}{\partial s}\frac{\partial \theta_3(s,t)}{\partial s},$$
$$g_3 \equiv -EA\frac{\partial^2 u_2(s,t)}{\partial s^2} + [EA - GA]\left[1 + \frac{\partial u_1(s,t)}{\partial s}\right]\frac{\partial \theta_3(s,t)}{\partial s}. \tag{A.5}$$

The rotatory component is given by

$$L_{\mathrm{ELR}} \equiv q_0 + q_1\cos^2(\theta_3(s,t)) + q_2\sin(\theta_3(s,t))\cos(\theta_3(s,t)) + q_3\sin^2(\theta_3(s,t)) + q_4\cos(\theta_3(s,t)), \tag{A.6}$$

where

$$q_0 \equiv -EI\frac{\partial^2 \theta_3(s,t)}{\partial s^2},$$
$$q_1 \equiv [EA - GA]\left[1 + \frac{\partial u_1(s,t)}{\partial s}\right]\frac{\partial u_2(s,t)}{\partial s},$$
$$q_2 \equiv EA\left[1 + \frac{\partial u_1(s,t)}{\partial s}\right] - [EA - GA]\left[1 + \frac{\partial^2 u_1(s,t)}{\partial s^2} - \frac{\partial^2 u_2(s,t)}{\partial s^2} + 2\frac{\partial u_1(s,t)}{\partial s}\right],$$
$$q_3 \equiv -[EA - GA]\left[1 + \frac{\partial u_1(s,t)}{\partial s}\right]\frac{\partial u_2(s,t)}{\partial s},$$
$$q_4 \equiv -EA\frac{\partial u_2(s,t)}{\partial s}. \tag{A.7}$$

Acknowledgements

This work was supported in part by a grant from the US Army Research Office through the Science Applications International Corporation. The author is the PI and Dr. Gary Anderson is the grant monitor.

References

1. Rosenberg, R. M., 'Normal modes of non-linear dual mode systems', *Journal of Applied Mechanics* 1960, 263–268.
2. Rosenberg, R. M., 'On the existence of normal modes of vibration of a nonlinear system with two degrees of freedom', *Quarterly of Applied Mathematics* **22**(3), 1964, 217–234.
3. Rand, R. H., 'A direct method for non-linear normal modes', *International Journal of Non-Linear Mechanics* **9**, 1974, 363–368.
4. Nayfeh, A. H. and Nayfeh, S. A., 'On non-linear modes of continuous systems', *Journal of Vibration and Acoustics* **116**, 1994, 129–136.
5. Vakakis, A. F. and Rand, R. H., 'Normal modes and global dynamics of a two-degree-of-freedom nonlinear system. I. Low energies', *International Journal of Non-Linear Mechanics* **27**(5), 1992, 861–873.
6. Kelly, A., 'On the Lyapunov center manifold', *Journal of Mathematical Analysis and Applications* **18**, 1967, 472–478.
7. Shaw, S. W. and Pierre, C., 'Normal modes for nonlinear vibratory systems', *Journal of Sound and Vibration* **164**, 1993, 85–124.

8. Mazzilli, C. E. N., Soares, M. E. S., and Baracho, N., 'Reduction of finite-element models of planar frames using non-linear normal modes', *International Journal of Solids and Structures* **38**, 2001, 1993–2008.
9. Bathe, K.-J., *Finite Element Procedures in Engineering Analysis*, Prentice-Hall, New Jersey, 1982.
10. Chung, T. J., *Applied Continuum Mechanics*, Cambridge University Press, New York, 1996.
11. Sirovich, L., 'Turbulence and dynamics of coherent structures', *Quarterly of Applied Mathematics* **45**, 1987, 561–571.
12. Georgiou, I. T. and Sansour, E., 'Analysing the finite element dynamics of nonlinear in-plane rods by the method of proper orthogonal decomposition', in *Computational Mechanics, New Trends and Applications*, S. Idelsohn, E. Onate, and E. Dvorkin (eds.), CIMNE, Barcelona, Spain, 1998.
13. Rubin, M. B., *Cosserat Theories: Shells, Rods and Points*, Kluwer Academic Publishers, Dordrecht, The Netherlands, 2000.
14. Sansour, C. and Bednarczyk, H., 'The Cosserat surface as a shell model, theory and finite element formulation', *Computer Methods in Applied Mechanics and Engineering* **120**, 1995, 1–32.
15. Georgiou, I. T., 'On proper orthogonal decompositions for one-dimensional coupled structural dynamics: Characterization of coupled vibrations in nonlinear elastic rods', 2004 (unpublished).
16. Feeny, B. F. and Kappagantu, R., 'On the physical interpretation of proper orthogonal modes in vibrations', *Journal of Sound and Vibration* **211**(4), 1998, 607–616.
17. Georgiou, I. T. and Schwartz, I. B., 1999, 'Dynamics of large scale coupled structural/mechanical systems: A singular perturbation/Proper Orthogonal Decomposition approach', *SIAM Journal of Applied Mathematics* **59**(4), 1999, 1178–1207.
18. Aubry, N, Holmes, P, Lumley, J. L., and Stone E., 'The dynamics of coherent structures in the wall region of a turbulent boundary layer', *Journal of Fluid Mechanics* **192**, 1988, 115–173.
19. Steindl, A. and Troger, H., 'Methods for dimension reduction and their application in nonlinear dynamics', *International Journal of Solids and Structures* **38**, 2001, 2131–2147.
20. Rega, G. and Alaggio, R., 'Spatio-temporal dimensionality in the overall complex dynamics of an experimental cable/mass system', *International Journal of Solids and Structures* **38**, 2001, 2049–2068.
21. Chidamparan, P. and Leissa, A. W., 'Vibrations of planar curved beams, rings, and arches', *Applied Mechanics Review* **46**(9), 1993, 467–482.
22. Georgiou, I. T. and Kanavis, C., 'A POD-Based identification of the reduced dynamics of an exact rod loaded transversely', in *Proceedings of DETC'03, ASME 2003 Design Engineering Technical Conferences and Computers and Information in Engineering Conference*, Chicago, IL, September 2–6, 2003.
23. Temam, R., *Infinite-Dimensional Dynamical Systems in Mechanics and Physics,* Springer-Verlag, New York, 1988.
24. Georgiou, I. T., 'Identification and construction of reduced order models for infinite-dimensional systems in nonlinear elastodynamics', in *Proceedings of IUTAM Symposium on Chaotic Dynamics and Control of Systems and Processes in Mechanics*, Rome, Italy, June 8–13, 2004.
25. Georgiou, I. T., Schwartz, I. B., Emaci, E., and Vakakis, A., 'Interaction between slow and fast oscillations in an infinite degree-of-freedom linear system coupled to a nonlinear subsystem: Theory and experiment', *Journal of Applied Mechanics* **66**, 1999, 448–459.
26. Georgiou, I. T. and Schwartz, I. B., 'Slaving the in-plane motions of a nonlinear plate to its flectural motions: An invariant manifold approach', *Journal of Applied Mechanics* **64**, 1997, 175–181.
27. Taylor, A. E. and Lay, D. C., *Introduction to Functional Analysis*, 2nd edn., Krieger, Malabar, FL, 1986.
28. Bowen, R. M. and Wang, C.-C., *Introduction to Vectors and Tensors: Linear and Multilinear Algebra*, Plenum Press, New York, 1980.
29. Jones, C., 'Geometric singular perturbations in dynamical systems', *Springer Lecture Notes Mathematics* **1609**, 1995, 44–120.
30. Georgiou, I. T., Corless, M. J., and Bajaj, A. K., 'Dynamics of nonlinear structures with multiple equilibria: A singular perturbation-invariant manifold approach', *Zeitschrift für angewandte Mathematik und Physik* **50**, 1999, 892–924.